Vitaly Golubev

Biofuel quality control
by portable XRF-analyser

Bachelor's Thesis
Environmental Engineering

May 2015

MAMK
University of Applied Sciences

DESCRIPTION

	Date of the bachelor's thesis May 11th, 2015
Author(s) Vitaly Golubev (email: astro.latlive@gmail.com)	**Degree programme and option** Environmental Engineering (B Eng)

Name of the bachelor's thesis

Biofuel quality control by portable XRF-analyser

Abstract

The objective of this thesis project was to find out feasibility of using a handheld XRF-analyser in solid biofuel quality control, particularly for recovered wood. Global biomass supply is estimated to grow rapidly, creating demand for automatic quality control systems. X-ray fluorescent technology brings about quick, accurate and non-destructive elemental analysis. Recovered wood fuel is challenging for combustion due to high levels of contaminants. During this work a list of challenging chemical elements in recovered wood fuel was created after reviewing relevant EU standards.

XRF technology has its limitations. Effects of limitations that are dependent on analysed samples were practically examined with an experimental XRF set-up built in a laboratory. As a result of the tests, it was found that increasing the XRF analysis time did not considerably improve the detected elemental concentrations. However an air gap between the analyser and a sample significantly decreased measured concentrations. Wood moisture also reduced detected concentrations although it could be possible to mathematically correct this effect if knowing the moisture content level. Another important finding was that analysing wooden matrix by hand with a handheld XRF-analyser posed health risks even if a backscatter shield was used, due to high dose rates of radiation scattered off the sample into surroundings.

In the conclusion, a handheld XRF-analyser can be utilised in solid biofuel quality control. Its accuracy can be further increased by compensating negative effects of known limitations.

Subject headings, (keywords)

XRF, analysis, biofuel, recovered wood, quality control, limitations, testing.

Pages	**Language**	**URN**
51	English	

Remarks, notes on appendices

Tutor	**Employer of the bachelor's thesis**
Aila Puttonen	Mika Muinonen Inray Oy Ltd (www.inray.fi)

CONTENTS

LIST OF ABBREVIATIONS

CCA   Chromated Copper Arsenate

DIY   Do It Yourself

EDXRF   Energy Dispersive X-Ray Fluorescence

GOLDD   Geometrically Optimized Large Drift Detector

LOD   Limits of Detection

MDF   Medium Density Fibreboard

OSB   Oriented Strand Board

PAS   Publicly Available Specification

RWW   Recovered Waste Wood

SDD   Silicon Drift Detector

SRF   Solid Recovered Fuel

WDXRF   Wavelength Dispersive X-Ray Fluorescence

WRAP   Waste and Resources Action Programme in United Kingdom

XRF   X-Ray Fluorescence

1   INTRODUCTION

Biomass has long been used for global heating. Combustion of biomass produces fewer emissions compared to fossil fuels, and it poses less ecological impacts. It can also be argued that biomass can be seen as a renewable source of energy. Understandably, biomass is increasingly becoming an important part of energy supply, especially for industrial uses.

In 2009, biomass shared 10,2 % of global energy supply, of which 13,5 % were used in industrial production of heat and power (Vakkilainen et al. 2013). It is estimated that by 2030 the demand for biomass will double (International renewable energy agency 2014). Therefore, more trade of biofuels will take place, and consequently, there will be a greater need for technologies to assess biomass quality.

Suppliers of solid biofuel are bound to provide specifications of their product. However, often fuel is sold for a higher price than its actual market value, for example, due to a greater concentration of pollutants than provided in the specifications. Therefore, there is a great interest and demand for equipment that could provide a fast and reliable fuel quality control.

An existing technology for solid fuel quality control is to send fuel samples to a laboratory for analysis. It is time-consuming and may be expensive in a long term. The X-ray Fluorescence (XRF) technology brings about high quality, fast and non-destructive measurements of fuel samples on site.

This thesis project was a preliminary study on feasibility of using a handheld XRF-analyser for solid biofuel quality control, particularly for recovered demolition wood. The thesis consisted of theory and practical work. The theory covered an overview of global bioenergy production, properties of recovered wood fuel and its classifications, description of the XRF technology, its limitations and current applications in solid biofuel quality control. The theory was obtained from previous publications and research as well as from different public web-resources of XRF-equipment manufacturers. The practical work was done with a handheld XRF-analyser in a laboratory at Mikkeli University of Applied Sciences, Finland. The aim was to test how measurement time, distance to a sample, and wood moisture affected the results of XRF analysis. The radiation rate doses during the testing were checked, and radiation safety was ensured. The thesis was commissioned by Inray Oy Ltd company.

2   GLOBAL BIOFUEL PRODUCTION

Biofuel is fuel derived from biological material, such as biomass, in forms of solid, liquid or gas. Solid biofuel mainly include wood, peat, forest residues, sawdust, animal manures and crops. Compared to conventional fossil fuels that are extracted and shipped worldwide, biomass is typically produced and consumed locally, and on a small scale.

In 2009, biomass was accounted for 10,2 % of global energy supply as shown in the Table 1. 65,4 % of biomass was consumed for residential use such as for heating and cooking while 34,6 % was utilised in industries. More detailed information is summarised in the Table 2. With regards to the geographical distribution of global biomass usage, around two thirds are used in developing countries (mostly residential use), and the rest is in developed countries (mostly industrial use). (Vakkilainen et al. 2013.)

TABLE 1. Global energy supply in 2009 (Vakkilainen et al. 2013)

Fuel type	Energy, EJ	% share
Oil	171	33,6
Coal	138	27,1
Natural gas	106	20,8
Biomass	52	10,2
Nuclear	29	5,7
Hydropower	12	2,4
Other	1	0,2
Total	509	100,0

TABLE 2. Global biomass supply in 2009 (Vakkilainen et al. 2013)

Usage	Energy, EJ	% share	Usage category	Energy, EJ	% share
Industrial use	18	34,6	heat and power generation	7	13,5
			industry	8	15,4
			transportation	2	3,8
			other	1	1,9
Residential use	34	65,4			
Total:	52	100,0			

The international renewable energy agency estimates that the global bioenergy demand will almost double by year 2030, from 53 EJ in 2010 to 108 EJ in 2030. Particularly, the growth will be high in the heat and power generation industry which will expand to around one third of total global biomass consumption by 2030. (International renewable energy agency 2014.)

3   RECOVERED WOOD FUEL

Recovered wood fuel is defined as wood material received from different categories of waste as fuel for heat or electricity generation. Wood waste sources may be grouped into 3 sectors: domestic sector, construction and demolition sector, and commercial and industrial sector (wooden packaging, wood products manufacture, treated timber products). (PAS 111:2012.)

3.1   Characteristics

Solid recovered fuel (SRF) includes all material mixes that can be incinerated and are certified according to the EN 15359 standard "Solid recovered fuels – specifications and classes". The source of SRF is mainly municipal solid waste, commercial and industrial wastes. Typical composition of SRF is as follows (in wet weight %): paper: 40-50 %, plastics: 25-35 %, and textiles: 10-14 %. In literature, solid recovered fuel category often includes recovered wood fuels. (Bankiewicz 2012; Jones 2013.)

Recovered waste wood (RWW) is all wood-based material which originates from waste and is intended to be processed for further use. It mainly comes from construction and demolition processes. In addition to wood material, RWW typically contains metal parts (nails, wires), plastics (flooring, electrical wires), paints and wood preservation treatments (CCA, creosote). The Table 3 below summaries different contaminants found in recovered waste wood. (Bankiewicz 2012; Jones 2013.)

TABLE 3. Recovered waste wood contaminants (Bankiewicz 2012)

Contaminant	Share, wet weight %
Surface treated wood	15
Preservative treated wood	3,5
Soil	0,6
Plastics	0,1
Iron, steel	0,5
Concrete	0,05

With regards to the chemical composition, RWW is problematic due to the high concentration of heavy metals, particularly Cr, Cu, Zn, Cd, Hg, Pb. Paints, lacquers, binders and preservatives contribute to the problem of heavy metals the most. SRF is reported to be high in chlorine and bromine because of plastics present in the fuel made from municipal waste. (Bankiewicz 2012, Vainikka 2011; Jones 2013.)

3.2 EN classification

This chapter is divided into 3 parts where each part is a review of a standard for solid biofuel classification. Firstly, EN ISO 17225-1:2014 focuses on classification and specification of biofuel with amount of halogenated organic compounds and heavy metals not exceeding the values of virgin wood. Secondly, EN 15359 gives classification for solid recovered fuel. Lastly, a specification PAS 111:2012 (UK) is also described.

EN ISO 17225-1:2014

The recent standard EN ISO 17225-1:2014 on specifications and classes of solid biofuels is binding for the European Committee for Standardization (CEN) members to adopt it to their national legislation. The standard is only intended for solid biofuels, including chemically treated wood, that do not contain halogenated organic compounds or heavy metals in amounts greater than those of typical virgin wooden material or virgin wooden material of a place of wood origin. If these elements exceed the norm, then the standard EN 15359 should be used for recovered wood classification instead. The Table 4 summarises concentration variations of elements in virgin coniferous wood given in the standard. For Cl the values are given in percentage of sample's dry weight. The Table 5 below shows classification of origin and source of recovered wood.

TABLE 4. Properties of virgin coniferous wood, ppm dry weight (ISO 17225-1:2014)

Element	Z	Without or with insignificant amount of bark, leaves and needles		Logging residues	
		Typical value, ppm dry basis	Typical variation, ppm dry basis	Typical value, ppm dry basis	Typical variation, ppm dry basis
Na	11	20	10 – 50	200	75 - 300
S	16	<200	<100 - 200	<200	<200 - 600
Cl, weight %	17	0,01	<0,01 – 0,03	0,01	<0,01 – 0,04
K	19	400	200 – 500	2000	1000 - 4000
V	23	<2	<2	0,6	0,1 - 1
Cr	24	1,0	0,2 – 10,0	1	0,7 - 1,2
Mn	25	150	100 – 200	130	80 - 170
Ni	28	0,5	<0,1 – 10	1,6	0,4 - 3
Cu	29	2	0,5 – 10	10	10 - 200
Zn	30	10,0	5 – 50	20	8 - 30
As	33	<0,1	<0,1 – 1	0,6	0,2 - 1
Cd	48	0,1	<0,05 - 0,50	0,2	0,1 - 0,8
Hg	80	0,02	<0,02 - 0,05	0,03	-
Pb	82	2	<0,5 - 10,0	1,3	0,4 - 4

According to the EN ISO 17225-1:2014, specification of solid biofuels includes normative (compulsory) and informative (voluntary) properties. There are several criteria to specify solid biofuels:

1. origin;
2. traded form;
3. properties such as dimensions, moisture and ash contents.

Normative properties to be stated depend on the origin and traded form.

TABLE 5. Classification of origin and sources of recovered wood (ISO 17225-1:2014)

Origin	Source	Sub-source
1.2. By-products and residues from wood processing industry	1.2.1. Chemically untreated wood by-products and residues	1.2.1.1 Broad-leaf with bark 1.2.1.2 Coniferous with bark 1.2.1.3 Broad-leaf with bark 1.2.1.4 Coniferous with bark 1.2.1.5. Bark (from industry operation)
	1.2.2. Chemically treated wood by-products, residues, fibres and wood constitutes	1.2.2.1. Without bark 1.2.2.2. With bark 1.2.2.3. Bark (from industry operation) 1.2.2.4. Fibres and wood constituents
	1.2.3. Blends and mixtures	
1.3. Used wood	1.3.1 Chemically untreated used wood	1.3.1.1 Without bark 1.3.1.2. With bark 1.3.1.3. Bark
	1.3.2. Chemically treated used wood	1.3.2.1. Without bark 1.3.2.2. With bark 1.3.2.3. Bark
	1.3.3. Blends and mixtures	

The EN ISO 17225-1:2014 gives 21 major traded forms of solid biofuels and their typical particle sizes. Among them are wood chips (5 mm – 100 mm), hog fuel (varying size), logwood (50 cm – 100 cm), firewood (5 cm – 100 cm) and sawdust (1 mm – 5 mm). However, other forms which are not included in the standard are also possible to be used.

Specification of fuel properties is dependent on fuel's origin and traded form. For example, properties for wood chips and hog fuel are listed in the Table 6 below.

TABLE 6. Normative and informative properties for wood chips and hog fuel (ISO 17225-1:2014)

Property	Value
Normative for all wood:	
Dimensions (P), mm:	P16S, P16, P31S, P31, P45S, P45, P63, P100, P200, P300
Fine fraction (F), <3,15 mm weight-%:	F05 (≤5%), F10 (≤10%) ... F30 (≤30%), F30+ (>30%)
Moisture (M), weight-% as received:	M10 (≤10%), M15 (≤15%) ... M55 (≤55%), M55+ (>55%)
Ash (A), weight-% of dry basis:	A0.5 (≤0,5%), A0.7 (≤0,7%) ... A10 (≤10,0%), A10.0+ (>10,0%)
Informative for all wood:	
Net calorific value (Q), MJ/kg or kWh/kg as received, or energy density (E), MJ/m^3 or kWh/m^3 loose	Minimum value to be declared
Bulk density (BD), kg/m^3	≥150, ≥200 … ≥400, ≥450
Ash melting behaviour, °C	Should be declared
Normative for chemically treated wood 1.2.2 and 1.3.2, and informative for not chemically treated wood:	
Nitrogen (N), weigh-% of dry basis:	N0.2 (≤0,2%), N0.3 (≤0,3%)…N3.0 (≤3,0%), N3.0+ (>3,0%)
Sulphur (S), weight-% of dry basis:	S0.02 (≤0,02%), S0.03 (≤0,03%)…S0.10 (≤0,10%), S0.10+ (>0,10%)
Chlorine (Cl), weight-% of dry basis:	Cl0.02 (≤0,02%), Cl0.03 (≤0,03%)…Cl0.10 (≤0,10%), Cl0.10+ (>0,10%)

An example of fuel specifications may be as follows:

- Origin: Chemically treated used wood (1.3.2)

- Traded form: Wood chips

- Properties: Dimensions P45, Fine fraction F20, Moisture M20, Ash A1.5, Nitrogen N1.0, Sulphur S0.08, Chlorine Cl0.10, Bulk density BD400.

EN 15359

If recovered wood contains amount of halogenated organic compounds and heavy metals exceeding the values of virgin wood, the EN 15359 standard "Solid recovered fuels – specifications and classes" should be applied instead of EN ISO 17225-1:2014. According to EN 15359 standard, solid recovered fuel (SRF) is fuel derived from non-hazardous waste. If properties of solid fuel cannot be confirmed with EN 15359 standard, then this fuel cannot be classified as solid recovered fuel. The standard includes demolition waste wood. It gives 5 classes of SRF for incineration as shown in the Table 7. The purpose of EN 15359 is to quickly give a class of solid fuel according to its economical, technical and environmental information that are represented by net calorific value, chlorine and mercury respectively. (European recovered fuel organisation.)

TABLE 7. Classification of SRF according to EN 15359

Classification property	Statistical measure	Unit	Class				
			1	2	3	4	5
Net calorific value, NCV	Mean	MJ/kg (as received)	≥25	≥20	≥15	≥10	≥3
Chlorine, Cl	Mean	% dry basis	≤0,2	≤0,6	≤1,0	≤1,5	≤3
Mercury, Hg	Median	Mg/MJ (as received)	≤0,02	≤0,03	≤0,08	≤0,15	≤0,50
	80th percentile	Mg/MJ (as received)	≤0,04	≤0,06	≤0,16	≤0,30	≤1,00

There are normative and informative values of SRF used for specification in this standard. They are grouped into physical and chemical parameters. The Table 8 below provides a list of these properties.

TABLE 8. EN 15359 normative and informative parameters for SRF (Merlini 2013)

Normative physical	Particle form, particle size, ash content (% dry basis), moisture content (% as received) and net calorific value (MJ/kg as received/dry basis).
Normative chemical	Cl (% dry basis) and all heavy metals listed in the 2000/76/EC Waste Incineration Directive, namely Sb, As, Cd, Cr, Co, Cu, Pb, Mn, Hg, Ni, Ti and V, mg/kg on a dry basis.
Informative physical	Bulk density (kg/m^3), Content of volatile matter (%) and ash melting behaviour (°C)
Informative chemical	Al, C, H, N, S, (% dry basis); Br, F, PCB, Fe, K, Na, Si, P, Ti, Mg, Ca, Mo, Zn, Ba, Be, Se, (mg/kg dry basis)

PAS 111:2012

PAS 111:2012 is a Publicly Available Specification (PAS) designed to provide producers and end-users of waste wood in the United Kingdom with a tool to classify wood into several categories based on its quality. Waste wood is defined as any type of wood that has been discarded or is intended to be discarded. It should be noted that the PAS 111 is not a British standard, and other restrictions may apply such as from the 2000/76/EC Waste Incineration Directive. The Table 9 below summarises information on how to give a grade to waste wood. According to PAS 111:2012, there are 4 classification grades of waste wood:

"grade A" Clean recycled wood,

"grade B" Industrial feedstock,

"grade C" Fuel,

"grade D" Hazardous waste.

TABLE 9. Grades of waste wood (PAS 111:2012)

Grade	Description
A	Solid softwood and hardwood. Packaging waste, scrap pallets, packing cases and cable drums. Residues from the production of untreated product. May contain nails and metal fixings. Minor amounts of paint, and surface coatings.
B	May have 60 % of grade "A" material, plus building and demolition material and domestic furniture made from solid wood. May contain nails and metal fixings. Some paints, plastics, glass, grit, coatings, binders and glues. Limits on treated or coated materials as defined by the Waste Incineration Directive.
C	All materials given in "A" and "B" grades, plus fencing products, flat pack furniture made from board products and DIY materials. High content of panel products such as chipboard, MDF, plywood, OSB and fibreboard. May contain nails and metal fixings. Paints coatings and glues, paper, plastics and rubber, glass, grit as well as coated and treated timber (but non CCA or creosote)
D	Fencing, transmission poles, railway sleepers, cooling towers. Contains material with CCA treatment and creosote.

The following abbreviations are used the Table 9:

DIY – Do It Yourself

MDF - Medium Density Fibreboard

OSB - Oriented Strand Board

CCA - Chromated Copper Arsenate

3.3   Challenging chemical elements

Totally 19 elements of interest have been identified. Of those, 4 elements (Na, K, Br and Zn) are included due to their corrosive effect during combustion as found on literature reviews, and the other 15 elements are mandatory for solid biofuel quality assessment based on recovered wood classifications from the previous chapter. The Table 10 lists the identified elements and their source of information. Negative effects of several elements on combustion reactors are also discussed below.

TABLE 10. Elements of interest for recovered wood fuel quality control

#	Symbol	Element name	Atomic number, Z	Source of information
1	N	Nitrogen	7	EN ISO 17225-1
2	Na	Sodium	11	Bankiewicz 2012; Sandberg 2011
3	S	Sulphur	16	EN ISO 17225-1
4	Cl	Chlorine	17	EN 15359, EN ISO 17225-1
5	K	Potassium	19	Bankiewicz 2012; Sandberg 2011
6	V	Vanadium	23	EN 15359
7	Cr	Chromium	24	EN 15359, PAS 111:2012
8	Mn	Manganese	25	EN 15359
9	Co	Cobalt	27	EN 15359
10	Ni	Nickel	28	EN 15359
11	Cu	Copper	29	EN 15359, PAS 111:2012
12	Zn	Zinc	30	Bankiewicz 2012; Sandberg 2011
13	As	Arsenic	33	EN 15359, PAS 111:2012
14	Br	Bromine	35	Bankiewicz 2012; Vainikka 2011
15	Cd	Cadmium	48	EN 15359
16	Sb	Antimony	51	EN 15359
17	Hg	Mercury	80	EN 15359
18	Tl	Thallium	81	EN 15359
19	Pb	Lead	82	EN 15359

Chlorine

Chlorine is considered to be the most dangerous element for combustion reactors. Chlorine is common in biomass and present in relatively high concentration. At the superheated temperature zone (600 – 700 °C) chlorine forms gaseous compounds such as HCl and Cl_2 which react with iron and chromium in the reactor's steel causing it to corrode. (Viklund 2013; Valmari 2000.)

Potassium and sodium

Potassium, being an important plant nutrient, is a dominant alkali metal in biomass followed by sodium. In combustion reactor, they can react with chlorine to form very low melting temperature compounds thus creating favourable conditions for ash and soot formation at lower superheated temperatures. Ash causes fouling and corrosion of reactor's surface. (Bankiewicz 2012; Sandberg 2011.)

Bromine

Deposits of bromine compounds (KBr and NaBr) develop corrosion of boiler steel. Bromides may cause high temperature corrosion of furnace's steel as well corrosion of boiler surface at low temperatures more extensively than caused by chlorides. (Bankiewicz 2012; Vainikka 2011.)

Lead and zinc

Lead and zinc are both heavy metals, and they can react with chlorine and sulphur in a combustion reactor forming salt mixtures that have a low melting temperature. Due to the low melting temperature, they deposit on the boiler's heat exchanging surfaces inducing fouling and slagging as well as corrosive effects already at 300 – 400 °C. (Bankiewicz 2012; Sandberg 2011.)

4   XRF TECHNOLOGY

X-ray Fluorescence (XRF) is widely used for a non-destructive elemental analysis. Compared to other analytical techniques, XRF is fast and reliable, and it does not require sample preparation. Samples do not need to be dissolved or destroyed in other ways. There are Energy Dispersive and Wavelength Dispersive XRF-analysers, and they differ considerably in their properties. However, the XRF technology has its limitations, and thus it is essential to know when and how an XRF analysis may give incorrect measurement results.

4.1   X-Ray Fluorescence principle

X-ray fluorescence is a phenomenon observed when an X-ray shines on material and generates a secondary X-ray, called fluorescent. The Figure 1 below schematically illustrates the XRF principle. A primary X-ray originated from an X-ray source is beamed at the material sample and accidentally hits an electron in an atom, e.g. on the K-shell. This electron is ejected from its electron shell creating a vacant place which is immediately occupied by an electron from a higher energy shell, e.g. L-shell or M-shell. When the electron makes the transition between the shells, a photon is emitted forming electromagnetic radiation, namely fluorescent X-radiation. The fluorescent X-ray carries energy unique to each chemical element, therefore by examining the energy level it is possible to understand the elemental composition of the sample. The XRF technology utilises such principle to analyse materials. (Amptek Inc.)
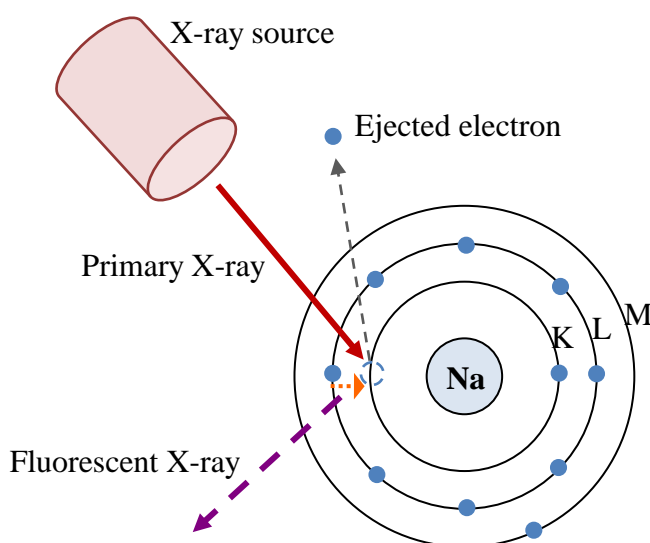
FIGURE 1. X-ray fluorescence principle

Additional letters alpha (α), beta (β) and gamma (γ) are used to classify the originating electron shell of fluorescent X-rays. An X-ray Kα is formed during the electron transition from the L-shell to the K-shell. An X-ray Kβ is created during the electron transition from the M-shell to the K-shell. Similarly, an X-ray Lα is emitted during transition from the M-shell to the L-shell. Moreover, there are several sub-levels in each electron shell, and every sub-level is distinguished by numbering. Therefore, X-rays are given labels such as Kα1 and Lβ2 for more detailed information on their origin. (Amptek Inc.)

4.2   Handheld XRF-analyser

The Niton XL3t 980 GOLDD+ is a handheld Energy Dispersive XRF-analyser (EDXRF) manufactured by Thermo Fisher Scientific Inc. It features an X-ray tube of 50 kV and 200 μA as an X-ray source as well as a large area Silicon Drift Detector (SDD) with resolution of less than 185 eV at 60 000 counts per second (Thermo Fisher Scientific Inc). Its analytical range of elements is from Mg to U. This portable XRF-analyser can be controlled either directly with a touch screen or remotely with computer software. The Figure 2 below illustrates the location of the X-ray tube and detector inside the analyser. Its software allows several analytical modes by default, of which TestAll Geo was used in this study.

FIGURE 2. Handheld XRF detection principle (left), and Niton XL3t 980 (right)

Analyser's radiation safety

In Finland, according to the guide on the "use of control and analytical X-ray apparatus" available from the Finnish radiation and nuclear safety authority, the effective annual radiation dose should not exceed 0,3 mSv. A human presence in the area with the dose rate over 1,5 µSv/h must be limited to one hour per day. Additionally, if the work is done in the area with the dose rate over 5 µSv/h, special safety procedure should be made to restrict the annual radiation dose to 0,3 mSv. (Finnish radiation and nuclear safety authority 2008.)

According to X-ray tube radiation survey certificate which is shipped along with the analyser, maximum radiation dose rates measured for a steel sample are as follows: at 5 cm distance it is 1,23 µSv/h while at 10 cm it is 0,36 µSv/h (Thermo Fisher Scientific Inc 2014).

4.3   Limitations of XRF analysis

Technologically, the XRF analysis gives different measurement results due to its limitations. There are several aspects that should be taken into consideration when measuring a concentration of particular elements.

Resolution of XRF equipment

The resolution of an XRF detector is a numerical value, measured in eV, which represents a difference between the nearest spectra peaks (K or L shells) of elements that the detector can recognise in a sample. For example, sodium has $K\alpha = 1,040$ keV and magnesium has $K\alpha = 1,254$ keV energies (Bruker). Their spectra peak difference is (1,254 - 1,040) keV = 0,214 keV, or 214 eV. If XRF equipment has a detector with a resolution greater than 214 eV, it will be problematic to distinguish between these two elements. (US Environmental Protection Agency 2004.)

There are 2 main types of XRF equipment architecture: Energy Dispersive XRF (EDXRF) and Wavelength Dispersive XRF (WDXRF). Their difference lies in the structure, accuracy and measurement time. The EDXRF is able to analyse the whole spectrum which is fast while the WDXRF focuses only on one element at a time which is very time consuming. After reviewing multiple XRF-analyser specifications from different manufacturers, it can be summarised that regarding the resolution, EDXRF ranges from 150 eV to 300 eV and above, while WDXRF has a resolution as low as 5 eV to 20 eV.

Elemental range

There is a range of elements that can be traced using the XRF technology. A typical EDXRF-analyser can identify elements from sodium to uranium (Bruker 2012). In comparison, a WDXRF-analyser is capable of distinguishing very light elements, from boron to uranium (Bruker 2012). Using the EDXRF technology, elements lighter than sodium are not detectable (Fellin et al. 2014), and elements lighter than argon are very difficult to detect because the energy levels of their fluorescent X-rays are low and fluorescent photons are weakened by the air gap between the sample and detector (Thermo Fisher Scientific Inc 2013). Because of these low energies, the fluorescent photons can be ejected from the sample only if the targeted atoms are close to the surface (Bruker 2008). Moreover, detectability of elements depends on other factors such as matrix composition, sample moisture and duration of measurements.

Measurement time

The measurement time is a crucial limit of the XRF technology. The longer the analysis time is, the more accurate the results are, because it produces more counts per second. Mathematically, if the measurement time is n-times longer, then the limit of detection (LOD) is improved SQRT(n)-times (Thermo Fisher Scientific Inc 2010). If a sample is analysed 4 times longer, the LOD will increase 2 times. Such dependence is also seen in the research made by Fellin at el. (2014) on wooden matrix using an Oxford Instruments X-MET 5100 EDXRF-analyser with an X-ray source of 45 kV 40 µA. The Table 11 below shows minimum detection limits of relevant to this study elements acquired from their work.

TABLE 11. Minimum detection limits (ppm) of elements in wood (Fellin et al. 2014)

Element	Atomic number, Z	Time, second								
		5	10	15	20	30	60	120	180	600
Cl	17	23000	16000	13000	11000	9000	7000	5000	4000	2000
K	19	20000	14000	12000	10000	8000	6000	4000	3000	2000
V	23	30	19	15	13	11	8	5	4	2
Cr	24	20	16	13	11	9	6	5	4	2
Mn	25	19	13	11	9	8	5	4	3	2
Co	27	15	11	9	8	6	4	3	3	1
Ni	28	15	10	8	7	6	4	3	2	1
Cu	29	23	16	13	11	9	7	5	4	2
Zn	30	20	14	12	10	8	6	4	3	2
As	33	12	9	7	6	5	4	3	2	1
Cd	48	29	21	17	15	12	8	6	5	3
Sb	51	59	42	34	29	24	17	12	10	5
Hg	80	3	2	2	1	1	0,8	0,6	0,5	0,3
Pb	82	2	2	1	1	1	0,7	0,5	0,4	0,2

Depth of analysis

There are 3 main variables that affect how deep X-rays penetrate a sample: energy of X-rays, density of the sample material, and energy level of analysed element. Firstly, the greater the energy of an X-ray photon from analyser is, the greater the measurement depth is.

Secondly, low density material matrix such as wood and plastic allow for a deeper X-ray screening, compared to denser material. Low-energy X-rays are not able to enter a high-density matrix and excite elements, while high-energy X-rays penetrate a low-density sample much deeper (Wobrauschek et al. 2010; Anzelmo et al. 2014). For example, in the mining industry, depending on a sample density, a typical range for XRF analysis is from several microns to 9,5 mm (Thermo Fisher Scientific Inc 2009).

Thirdly, the analysis depth is different for each element due to the elemental excitation energy. The higher the atomic energy of an element, the deeper it can be traced within a sample (Guthrie 2012; Anzelmo et al. 2014). With regards to the thickness of wood analysis, Fellin et al (2014) reported a maximum detection depth of copper (Cu) from 15 mm to 24 mm depending on wooden matrix.

Distance to sample

The distance between an XRF-analyser and sample attenuates the number of fluorescent X-ray photons (Wobrauschek et al. 2010). For the best performances it is suggested to have a direct contact with tested material (US Environmental Protection Agency 2004; Thermo Fisher Scientific Inc 2010). Naturally, having such a distance is crucial for online sorting systems where wood comes in different shapes and sizes. Therefore there must be a gap between the XRF-analyser and conveyer. In research on XRF analysis of CCA-treated wood conducted by Solo-Gabriele et al (2003) it was recommended mounting the analyser at a most practical distance of 19 mm above the belt, with the maximum distance for XRF being 30 mm.

Moisture

If the moisture of a sample is greater than 20 %, then it can negatively affect XRF-analysis results. The reason is water contained in the sample, or on its surface, which serves as an extra-barrier for X-rays. It is possible to calibrate an XRF analyser for more accurate analysis after correction factors are determined with help of a dried sample in a laboratory. (US Environmental Protection Agency 2004; Glanzman & Closs 2007.)

On the other hand, for CCA-treated wood, Solo-Gabriele et al. (2003) suggest that there was no significant difference in detecting arsenic in a wet sample after 30 minutes of soaking it in water compared to a dry sample (during 3 second test with a 19 mm air gap).

Particle size

Firstly, in natural matrix elements are not distributed equally, therefore large particles do not represent the whole sample. Secondly, heterogeneous matrix scatters fluorescent X-rays away from the XRF-detector which lowers the quantitative results of analysis. Graining to fine particles and making a homogeneous sample is highly recommended in order to acquire more accurate results. In case of fine homogeneous matrix, the X-rays could reach particles that are hidden behind the top particles' layer therefore making a more representative analysis. (Thermo Fisher Scientific Inc 2013; Anzelmo et al. 2014; Glanzman & Closs 2007.)

Spectral matrix effect

In addition to the above described limitations, there are 3 more that can cause false XRF-analyser's readings. Namely, those effects are overlapping, enhancement and absorption.

Overlapping of spectral lines occurs when analysed elements emit fluorescent photons of similar wavelength. For example, lead L-peak overlaps with arsenic K-peak. Moreover, if a proportion of lead to arsenic is at least 10:1, then concentration of arsenic cannot be measured adequately due to a complete overlap. (US Environmental Protection Agency 2004.)

During the enhancement, an XRF-analyser can show a higher concentration of several elements because their binding elemental energies are less than those of fluorescent X-rays of other elements present in a sample. In addition to the analyser's X-ray source, these fluorescent X-rays become a secondary source of X-rays for the elements with lower elemental energies. An example of this can be chromium enhanced by iron. (Thermo Fisher Scientific Inc 2013; US Environmental Protection Agency 2004.)

Lastly, there are several elements that absorb or scatter fluorescent X-rays of other elements, as it is in the case of iron absorbing copper fluorescent X-rays. The absorption causes an XRF-analyser to show lower concentration values of elements than there really are in the sample. Computer software of the analyser is designed to effectively correct these limitations. (Thermo Fisher Scientific Inc 2013; US Environmental Protection Agency 2004.)

4.4   Online XRF applications in wood fuel processing

Online XRF-systems are widely used in mining industry for quality assessment of extracted ores (Nakhaei et al. 2012). However, full-scale working implementations of online XRF-systems in wood fuel processing have not been found. There is a limited number of studies on online wood fuel XRF-analysis. Notably, a pilot project carried out by Solo-Gabriele et al (2001) for the Sarasota county, USA, looked at XRF-analysis for sorting of CCA-treated wood. It was found that XRF technology can be effectively used to detect CCA-treated wood from other types of wood pieces on a moving conveyer. One limitation of online measurement is that an XRF-analyser should be mounted above the belt at a distance thus reducing the quality of results. Moreover, a slow speed of XRF-analysis is also a limit because it slows down the conveyer and minimises the amount of analysed wood per given time. As a result, the optimal height above a belt was 19 mm, and the minimum sufficient time was 3 seconds. The measurement time can be dramatically reduced to milliseconds if the XRF-analyser is built specifically for online measurement and its shatter is constantly open. In addition, although paints, coating and stains on wood pieces were found to reduce number of As fluorescent X-ray counts, CCA-treated wood was still detectable. (Solo-Gabriele et al. 2001.)

Another field trial research on online sorting of treated wood was done in cooperation of Pöyry Forest Industry Consulting Ltd and Waste and Resources Action Programme in the UK, 2009. In online analysis, XRF technology was capable of identifying Cu in Tanalith treated wood with concentration above 40 mg/kg at 2,7 seconds on average. For CCA-treated wood, it was found that As and Cr will be easily traced with XRF while Cu analysis gave too high uncertainties for conclusive results at 6,2 second measurement time. Detection of clean wood takes long time duration (up to 30 seconds). As the concentration of elements increases, the analysis time decreases. In the end, as the report suggests, it is questionable if XRF technology can be effectively applied to an online recovered wood sorting of recovered wood due to the distance between an XRF-analyser and wood on a conveyer, different shapes of wood pieces and a long analysis time required. (Waste and Resources Action Programme 2009.)

5   METHODS USED IN THIS STUDY

The practical tests formed a preliminary study on XRF-analysis of recovered wood with emphasis on simulating conditions for an on-line XRF system. The limitations of the XRF technology were tested and observed, particularly, how length of analysis, measurement distance to a sample, and wood moisture affect results of the XRF-analyses.

The Niton XL3t 980 GOLDD+ analyser was fixed on a laboratory stand which allowed moving the device vertically with a 2 mm step. A backscatter shield was attached to the analyser. The analyser was remotely controlled with software on a laptop. In the beginning of the practical work radiation levels near the XRF-analyser were measured with a radiation detection meter because, being low-density material, wood did not absorb X-rays very well, unlike metal matrices, scattering them to the surroundings. The Picture 1 below illustrates the initial measurement set-up with the radiation meter in the centre. An improved set-up design included lead shielding installed to protect the workplace from the radiation, as seen in the Picture 4 (chapter 6.5 "Radiation safety").
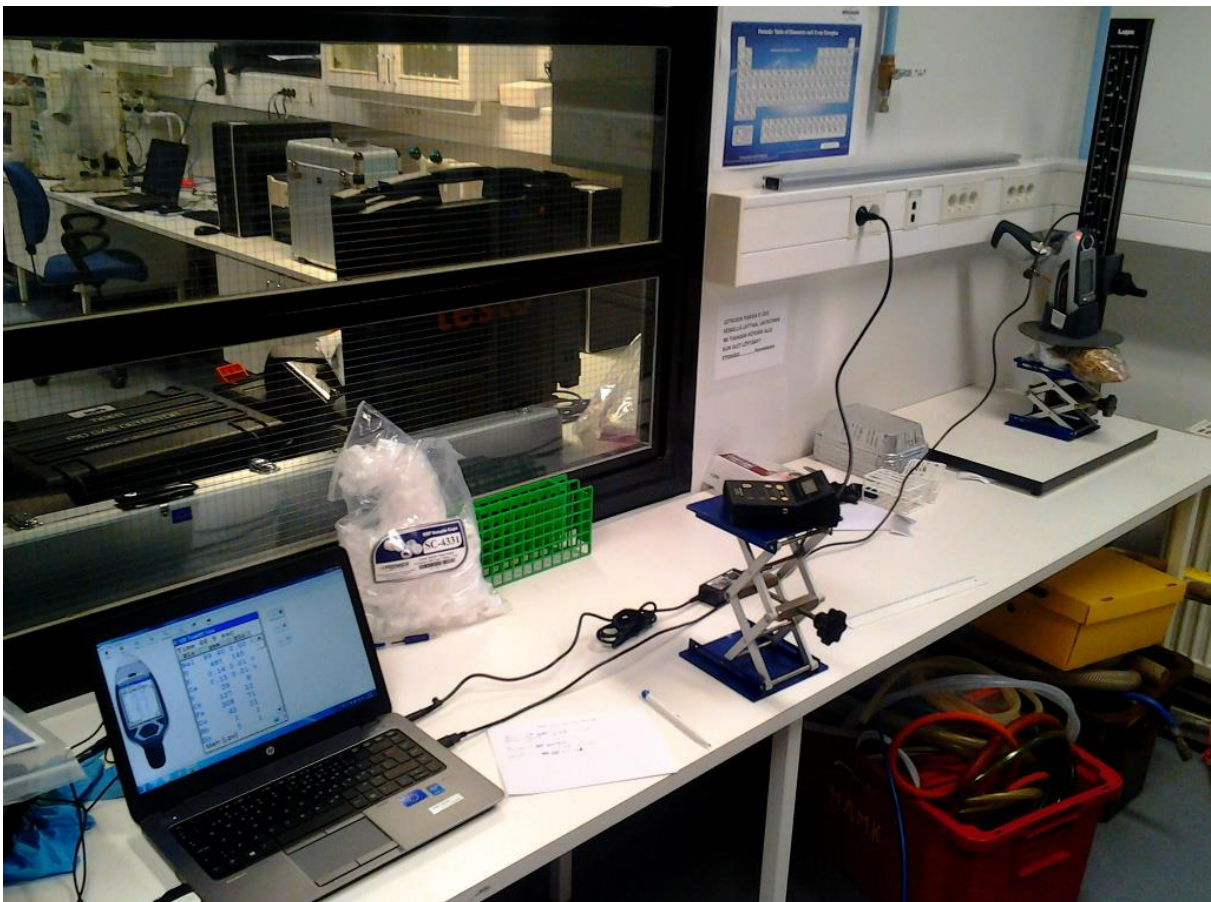
PICTURE 1. Initial set-up for XRF-analyser during radiation level measurements

For the radiation measurement, oven-dried wood chips in a plastic bag were chosen as a sample. The plastic bag was used because it was noticed that most of XRF analyses in the laboratory were done with plastic bags. The radiation check points were at 1 cm, 40 cm, 80 cm, and 120 cm distance to the analyser. The radiation detection meter was placed on a laboratory jack stand at the same height as the analysed sample, as seen in the Picture 1 above. Two sets of measurement were performed: when the analyser contacted the sample and when it was 2 cm above the sample. The analysis mode of the XRF analyser was set to "Soil" as soil is closer to wood by density than metal alloys. The radiation dose rate was observed to be the highest when the analyser worked in the "Main" elemental range of the chosen mode. The analysis time for this range was set to 1 minute to measure radiation in the vicinity.

During the practical work, performance of the handheld XRF-analyser was tested with wood samples that were in a form of recovered wood chips. They originated from a building demolition site. The chips were screened and separated to chip size groups of "≤ 1 mm", "≤ 2 mm", "≤ 4 mm", "≤ 8 mm", "≤ 12 mm", and "≤ 31,5 mm". For instance, the label "≤ 2 mm" means that this chip size group includes wood particles bigger than 1 mm and not bigger than 2 mm. The Picture 2 below shows the screened wood chip groups.

PICTURE 2. Demolition wood chip groups. From left to right, top to bottom: "≤ 1 mm", "≤ 2 mm", "≤ 4 mm", "≤ 8 mm", "≤ 12 mm", and "≤ 31,5 mm" chip size groups.

Wood chip samples were analysed in an aluminium foil container with bulk density and without a plastic bag in order to simulate real-life measurements on a conveyer in open air. The finest particles ($\leq$ 1 mm in size) were analysed in test cups provided with the XRF-analyser. Due to wood's low density, during the first trials it was checked whether the analyser made elemental analysis only of the sample or also detected elements of the sample container. It was observed that, at small sample size the analyser could detect not only the elements of the container but also some elements of the stainless steel laboratory jack which was used to hold the sample. Therefore the set-up was improved to ensure that only the sample was analysed, as shown in the Figure 3. Firstly, an empty plastic container was placed on the jack to create an air gap between the stand and sample to attenuate fluorescent photons emitted from the stand. Secondly, 7 mm of A4 paper sheets were placed on top of the plastic container to hold the sample. Paper sheets were chosen because they were not detected by the XRF analyser through the sample, and the sheets were strong enough to support the weight. Thirdly, enough layers of sample material were used to attenuate fluorescent X-rays emitted from the aluminium foil container. As a result, only the sample was analysed by the XRF-analyser. This design was kept during all practical work.
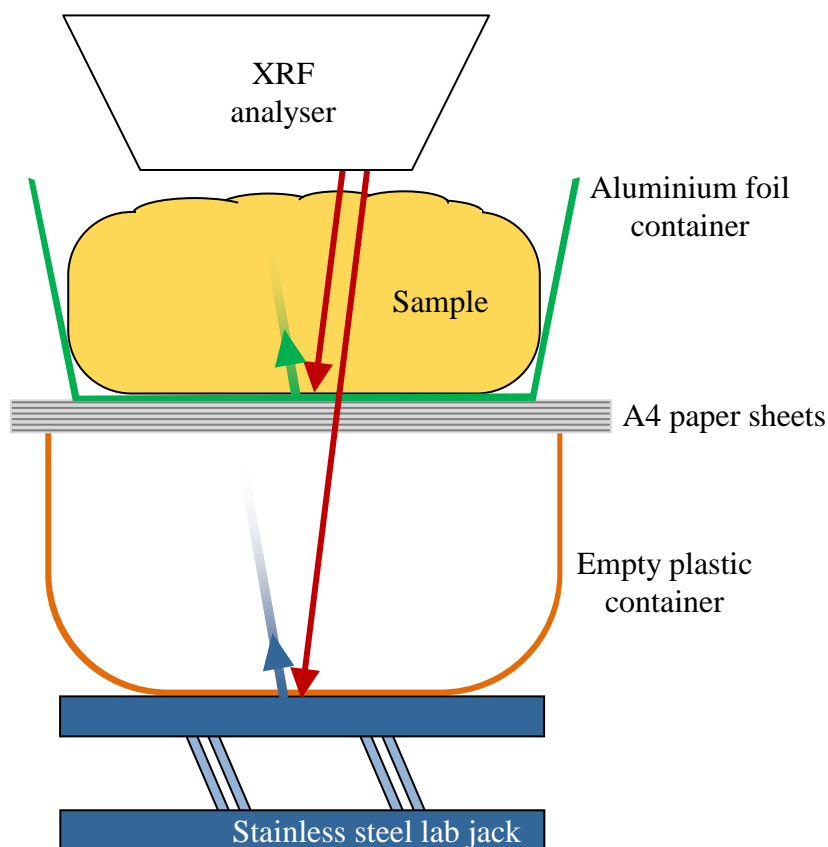
FIGURE 3. Stand design to attenuate fluorescent photons emitted from laboratory jack and sample container

Another challenging part was to evaluate raw measurement data received from the XRF-analyser as Microsoft Excel spreadsheet files. The spreadsheet size was too big for convenient analysis as it had the detected concentration values of 43 elements. Because typically during the practical work, there were only 10 detected elements of interest for this study, their values had to be copied from the original Excel file to another file for further analysis. Considering the fact that manual copying of data was inconvenient, very slow, and it could lead to copying wrong values, a data copying application was developed within Microsoft Excel in order to ease working with the raw XRF data. The application interface is shown in the Picture 3 below. This application made 100 % accuracy during the copying, and it dramatically increased the data processing speed.
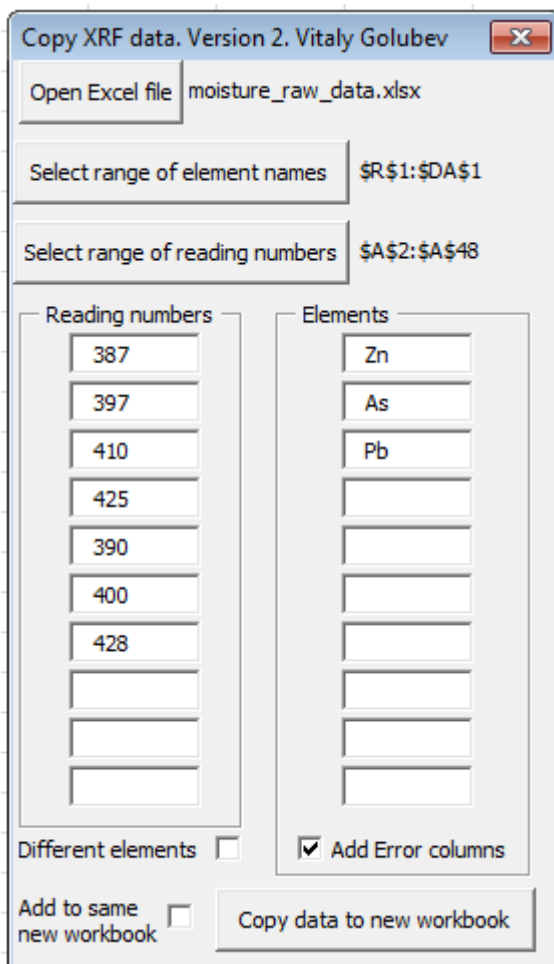
PICTURE 3. MS Excel application designed to extract XRF analysis data

With regards to the demolition wood chips, they had a very strong odour and high concentration of harmful elements. Therefore a breath mask and rubber gloves were worn all the time, and goggles were additionally used when working with small size particles ("≤ 1 mm", "≤ 2 mm"). The laboratory room was constantly ventilated during the practical work.

The XRF-analyser allowed working in different pre-set testing modes. For this study the mode "TestAll Geo" was chosen because in this mode the analyser could detect all elements, including light elements. Other available modes focused on analyses for specific applications, leaving out several elements from the analysis. The working principle of the analyser was that it divided all elements into ranges and sequentially measured elements of each range. In the "TestAll Geo" mode, there were 4 element ranges: light, low, main, and high range. It was possible to adjust duration of measurement for each range. All element ranges were set to equal analysis time. For convenience in this study, for example, in figures and tables, the measurement time corresponds to the analysis time per element range. For instance, a 15 second measurement time is a time that the XRF-analyser needs to analyse a range. In this case the total measurement time needed to analyse all elements is 15 seconds x 4 ranges = 60 seconds. The analyser took about 0,25 second to switch between the ranges.

With regards to limitations of this study, the most important one is that there were no other means of checking elemental concentrations found with the XRF analysis. However, the analyser was periodically controlled with a Standard Reference Material 2709a available from the US National Institute of Standards and Technology. This standard was dry soil, and all the control tests were within the standard deviation range given by the manufacturer. Therefore, it is confident to say that XRF analysis performed on recovered wood samples is accurate. The latest factory quality control of the analyser prior this study was performed on 11 November 2014.

6   PRACTICAL TEST RESULTS

In the tables below the results are expressed in ppm (parts per million). An empty cell means that an element was not detected by the XRF-analyser. The colours indicate an elemental concentration, where red colour is the highest value and green colour is the lowest value. Other colours highlight concentration values between the highest and lowest values.

The XRF analysis results are given with a measurement error, which is two standard deviations, also known as two-sigma. The result with this error is at around 95 % confidence level. It means that, for instance, if a concentration of Cl was measured to be 1500 ppm with the two-sigma error of ±30 ppm, there is a 95 % probability that the true Cl concentration value is between 1470 ppm and 1530 ppm. All XRF measurements errors in this study correspond to the two-sigma error. (Thermo Fisher Scientific Inc 2010.)

6.1   Particle size and chemical composition

Around 0,5 kg of sample were screened during 5 minutes for size distribution. This sample material was used for all following XRF-analyses. The results are presented in the Figure 4. The most common chip size is between 8 mm and 12 mm accounting for around 23 % of wet weight. The moisture content of the whole batch was 16,3 %.
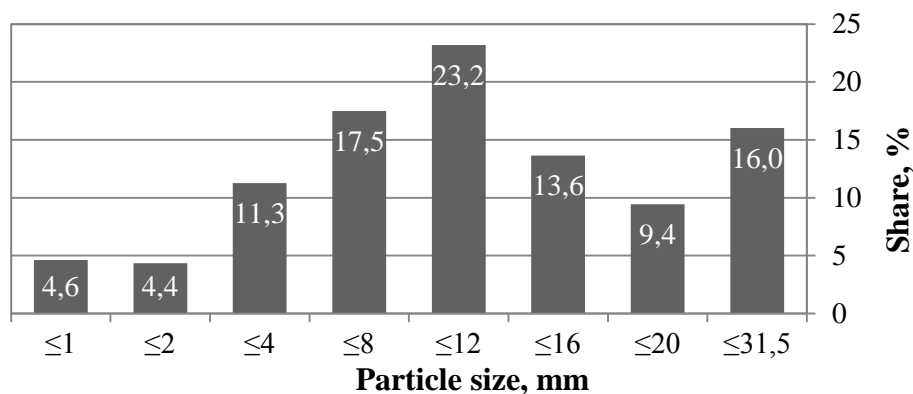
FIGURE 4. Particle size distribution of recovered wood sample by wet weight

For XRF analyses, all particles over 12 mm were combined together to form a group ≤ 31,5 mm. Totally, there were 6 size groups. The Table 12 shows the bulk density of each group, and moisture of selected groups. The "original mix" corresponds to the unsorted raw sample. The particles with the highest bulk density were the finest particles (≤ 1 mm).

TABLE 12. Bulk density of recovered wood samples

Particle size, mm	Bulk density, kg/m³	Moisture, %
≤1	230	21,9
≤2	180	
≤4	170	27,1
≤8	190	
≤12	200	
≤31,5	200	22,4
Original mix	190	16,3

The Table 13 below provides results of XRF elemental analyses of particles of different sizes. For this test, 3 representative samples were taken from each size group, and they were analysed during 60 seconds per element range. The values shown in the table are the average of these 3 samples. "St. dev" corresponds to a standard deviation between the concentration values of the 3 samples. "St. dev" is not the two-sigma error. "N/A" indicates that only one sample contained the element and the other two did not, thus it was not possible to calculate the standard deviation. It was found that the small wood particles had a higher concentration of contaminants than the bigger wood chips. The reason for this could be that the small particles, especially the finest (≤ 1 mm), compared to the bigger wood chips, contained higher concentrations of particles that were formed by detached paint and treated surface layers.

TABLE 13. XRF analysis of different particle size groups

Particle size, mm	≤ 1	≤ 2	≤ 4	≤ 8	≤ 12	≤ 31,5
Element	Concentration, ppm					
S	11927,44	6587,69	9357,56	4536,68	6176,25	3168,85
S st. dev	1737,00	544,67	2649,63	1024,97	4786,53	910,06
Cl	1498,83	960,11	1101,85	728,46	590,52	504,74
Cl st. dev	246,52	193,78	150,66	311,44	286,02	157,78
K	3685,48	1996,79	2073,67	1426,90	1074,75	1041,46
K st. dev	1132,95	294,27	134,73	246,98	125,17	267,71
Cu	66,33	48,04	31,78	22,19	38,70	16,38
Cu st. dev	5,39	15,26	5,74	1,43	18,18	N/A
Zn	462,40	174,17	118,79	65,70	44,94	36,71
Zn st. dev	79,31	10,82	16,05	25,75	18,61	16,03
As	47,95	16,04	10,01	9,76	24,33	3,39
As st. dev	6,99	3,93	2,00	7,91	N/A	N/A
Pb	423,99	79,79	54,75	63,93	24,51	15,65
Pb st. dev	15,91	8,07	4,53	42,49	9,04	2,15
V	56,52			8,89		
V st. dev	14,33			N/A		
Cr	67,27			37,17	60,46	
Cr st. dev	1,92			N/A	N/A	
Mn	146,16					
Mn st. dev	22,55					

6.2 Measurement time

How measurement time affects the XRF-analyser's results may be seen in the Table 14. The evaluation was done of the finest (≤ 1 mm) particles at one spot at different time lengths. The 60 second analysis was conducted 3 times, and all the other measurements were conducted 10 times. The values in the table are the average of the measured concentrations.

TABLE 14. Detection of elements at different measurement times for ≤ 1 mm particles

Time, s	4	5	10	15	20	30	60
Element	Concentration, ppm						
S	12557,02	11893,71	12205,77	12680,93	13106,20	13404,74	13594,64
S error	3641,01	1025,34	418,71	289,33	241,51	190,55	128,59
Cl	1433,97	1461,76	1421,26	1454,98	1494,13	1544,06	1570,18
Cl error	848,48	240,33	94,80	64,08	53,00	41,65	27,88
K	4897,64	4284,64	4421,88	4610,15	4722,49	4903,61	4983,30
K error	824,06	622,20	324,92	255,35	208,91	165,44	113,59
V					63,95	69,66	66,76
V error					41,14	29,21	19,91
Cr					46,95	54,37	57,86
Cr error					22,18	16,97	11,57
Mn			117,18	122,64	144,69	147,44	154,45
Mn error			60,38	44,46	38,34	30,77	21,59
Cu	62,59	56,13	54,01	57,11	58,89	59,36	60,94
Cu error	35,76	39,64	17,75	13,67	11,58	9,30	6,51
Zn	507,71	481,82	473,01	482,02	515,94	524,91	541,15
Zn error	50,26	49,72	27,02	20,74	18,00	14,54	10,27
As	48,96	46,20	37,96	38,72	41,69	42,09	41,08
As error	39,04	34,73	15,44	11,83	10,21	8,21	5,74
Pb	420,87	403,66	396,62	402,77	423,59	426,08	430,42
Pb error	42,54	42,29	23,03	17,65	15,18	12,20	8,54

Interestingly, the results above indicate that there was no significant difference between different analysis times. On average, the lowest detected concentration value represents 85 % of the maximum concentration value. It is also practically seen that the two-sigma analysis error decreased logarithmically as given in the literature (Thermo Fisher Scientific Inc 2010). The Figures 5, 6, and 7 illustrate how the measurement time affected the results of XRF analysis for Cl, K, and Pb respectively.
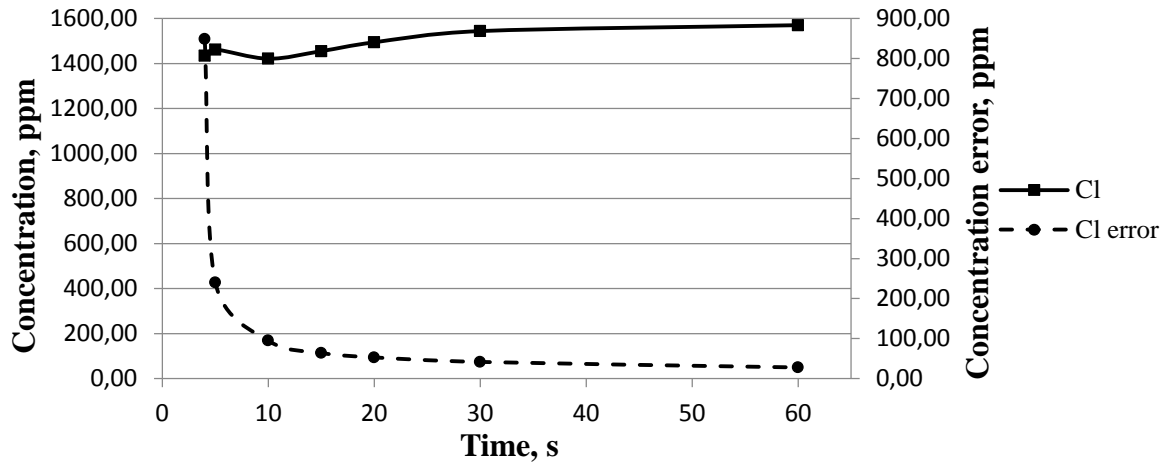
FIGURE 5. Dependence of Cl detection and analysis error on measurement time
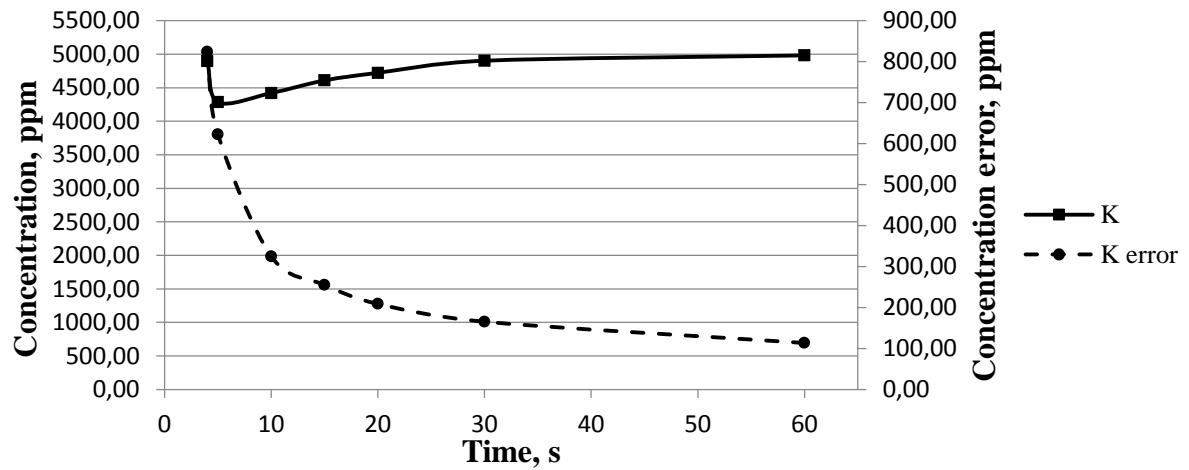
FIGURE 6. Dependence of K detection and analysis error on measurement time
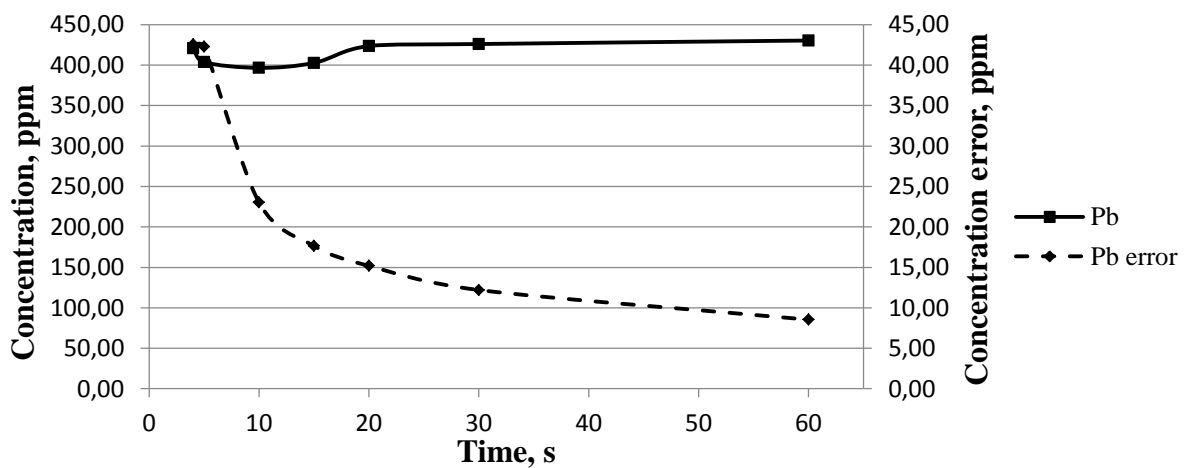
FIGURE 7. Dependence of Pb detection and analysis error on measurement time

6.3 Measurement distance

The depths of analysis in recovered wood (for ≤ 12 mm particles) at different distances above a sample are summarised in the Table 15. It was found using a plastic bag filled with pure iron powder under the recovered wood sample. Multiple 15 second measurements were carried out in order to identify Fe at a contact with the sample, at 1 cm and 2 cm above it. Wood particles were added to increase the analysis depth if Fe was still identified during the measurements.

TABLE 15. Depth of XRF analysis of Fe at different distances to sample

Air gap, mm	Analysis depth, mm
0	25
10	20
20	15

For an online XRF measurement system over a belt, it is necessary to have a distance between the analyser and moving materials. Therefore, an influence of an air gap between the XRF-analyser and a sample (the ≤ 4 mm particles) was studied. The same spot was tested 4 times at different time durations and distances. The average values are available in the Table 16 below.

TABLE 16. Detection of elements at different measurement distances to sample and analysis times, for ≤ 4 mm particles

Time, s	5 s			10 s			15 s		
Air gap	0 mm	10 mm	20 mm	0 mm	10 mm	20 mm	0 mm	10 mm	20 mm
Element	Concentration, ppm								
S	2308,20	1437,42	511,34	6595,26	642,26	399,75	6902,11	618,69	455,22
S error	894,95	539,83	227,32	338,78	194,76	122,97	254,56	137,21	98,51
Cl		1721,95		1387,04	671,86		1447,77	669,91	
Cl error		2129,69		103,29	1491,05		76,98	2137,95	
K	2617,34	937,21	745,43	2768,71	1030,57	720,73	2868,25	982,25	764,98
K error	382,74	166,08	110,67	230,48	94,93	65,00	163,24	66,76	50,60
Zn	121,11	83,63		128,04	73,96		125,52	78,41	
Zn error	33,11	70,45		17,79	32,55		13,26	23,79	
Pb	53,45	56,86		54,19	59,00		54,03	53,03	48,87
Pb error	19,13	29,67		10,15	20,96		7,62	14,86	24,09
Cu				44,30			42,58		
Cu error				20,37			15,24		
As							10,67		
As error							6,22		
V									
V error									
Cr			20,71			20,20		16,72	20,29
Cr error			10,44			6,18		7,41	4,68

TABLE 16. Detection of elements at different measurement distances to sample and times for ≤ 4 mm particles (continues)

Time, s	20 s			30 s			60 s		
Air gap	0 mm	10 mm	20 mm	0 mm	10 mm	20 mm	0 mm	10 mm	20 mm
Element	Concentration, ppm								
S	6890,40	613,91	373,46	7681,12	645,04	417,29	7234,20	634,83	435,52
S error	212,18	114,82	79,22	164,38	92,05	65,72	106,55	62,36	45,25
Cl	1467,25	703,87		1633,80	661,29		1541,81	722,37	
Cl error	64,54	1591,83		49,04	1995,27		32,06	1242,60	
K	2956,30	1002,04	787,10	3412,40	1009,71	782,36	3150,55	1012,00	747,08
K error	137,28	56,33	44,68	112,66	44,51	35,33	76,48	30,35	23,42
Zn	136,97	80,49	71,80	139,80	91,16	66,73	134,32	89,94	61,74
Zn error	11,22	20,53	37,77	9,31	17,10	17,66	5,99	11,48	20,36
Pb	57,21	62,00	54,54	56,84	59,75	66,73	55,08	60,09	68,03
Pb error	6,37	13,42	21,58	5,22	10,58	17,66	3,39	7,16	12,54
Cu	37,79			35,95			36,92		
Cu error	12,27			10,06			6,59		
As	10,95			13,39			12,53		
As error	5,19			4,32			2,79		
V						5,04		6,12	5,61
V error						2,57		2,97	1,76
Cr		15,05	23,02		17,14	22,07		16,47	22,10
Cr error		6,18	4,16		4,91	3,28		3,33	2,23

In this test, the most accurate result was acquired during a 60 second measurement at a 0 mm distance to the sample because the analysis error logarithmically decreased with time and there was no air gap that attenuated fluorescent X-rays. It was not possible to measure above 20 mm because there were not enough counts per second for the XRF-analyser to detect elements. It produced an error and caused the analyser to stop the tests.

Analysing the above given results, it can be concluded that the air gap changed the detected elemental concentration very much, especially for light elements. For example, for a 60 second measurement if the XRF-analyser was lifted 10 mm above the sample, it measured S concentration to be 1/11 of the value acquired during the contact measurement. Cl was not identified at 20 mm distance at all. However, V and Cr were detected at 10 mm and 20 mm distances even though the analyser did not identify these elements at the contact measurement. It probably occurred because at these distances the detection errors were too high and the analyser misanalysed the concentration of these elements. Elements Cu and As were not identified at any of the tested air gaps, probably due to their low concentrations.

A more extensive testing was conducted in order to find any possible dependence of element detection on the elevation distance. Two samples were analysed: oven-dried ≤ 8 mm particles, labelled "a", and oven-dried 6 mm particles received by grinding the ≤ 31,5 mm particles, labelled "b". Three different spots of each sample were analysed, labelling the spots, for example, as "a1" or "b2". The XRF-analyser was elevated above the samples with a step of 2 mm. The measurement time was set to 5 seconds per element range. 2 measurements were taken at each elevation distance, and their average value was used for the calculation. Because the analysis results were received in ppm, in order to compare all the measurements regardless of their real elemental concentration and find a possible trend, the data was converted to per cent. 100 % was set to be the concentration value detected at a 0 mm distance to the wood samples. The results of data analysis are presented in the following Figures 8 - 24 below.
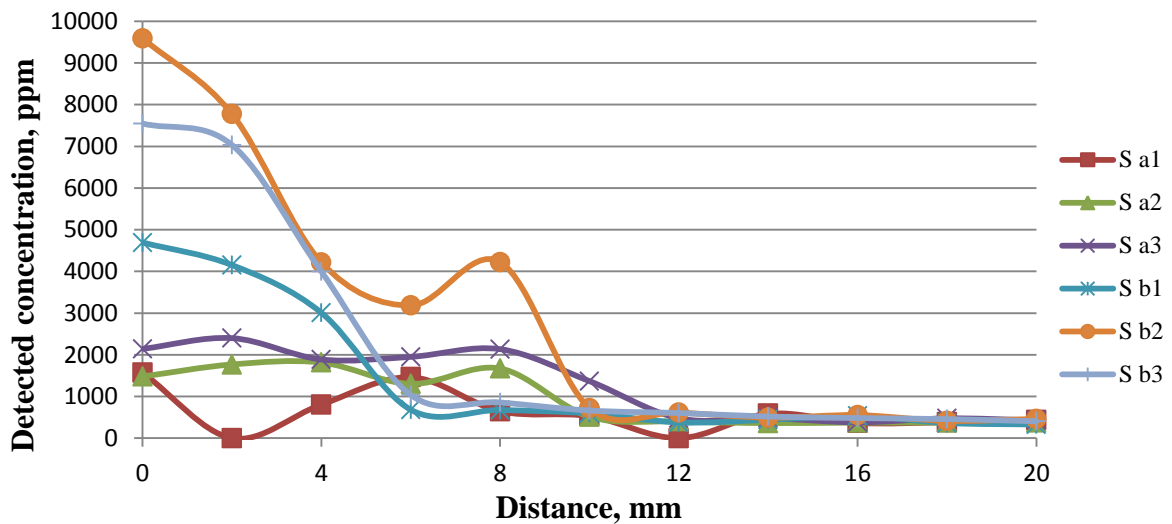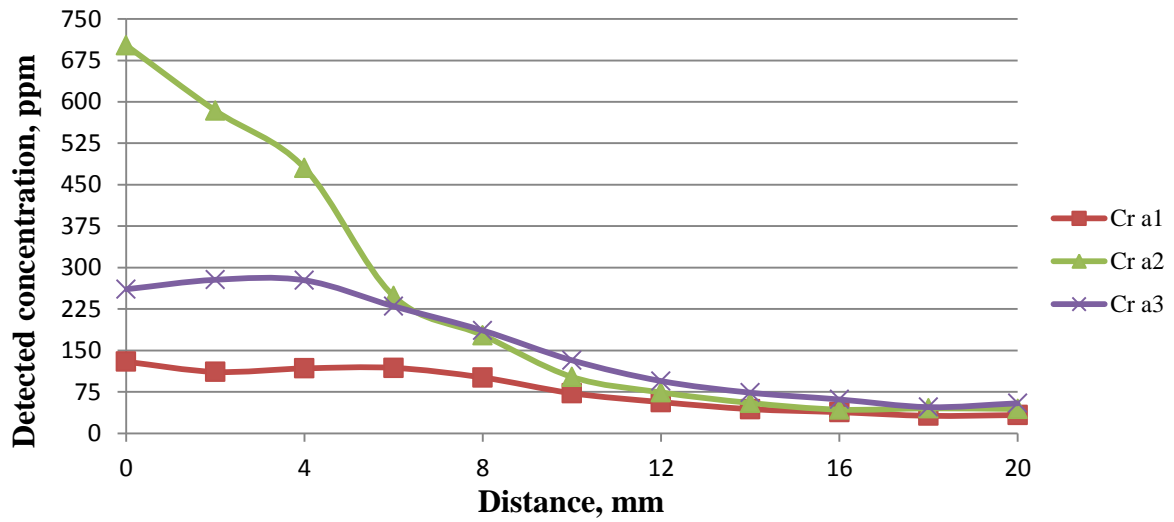

FIGURE 8. Dependence of detected S concentration on distance to sample, ppm
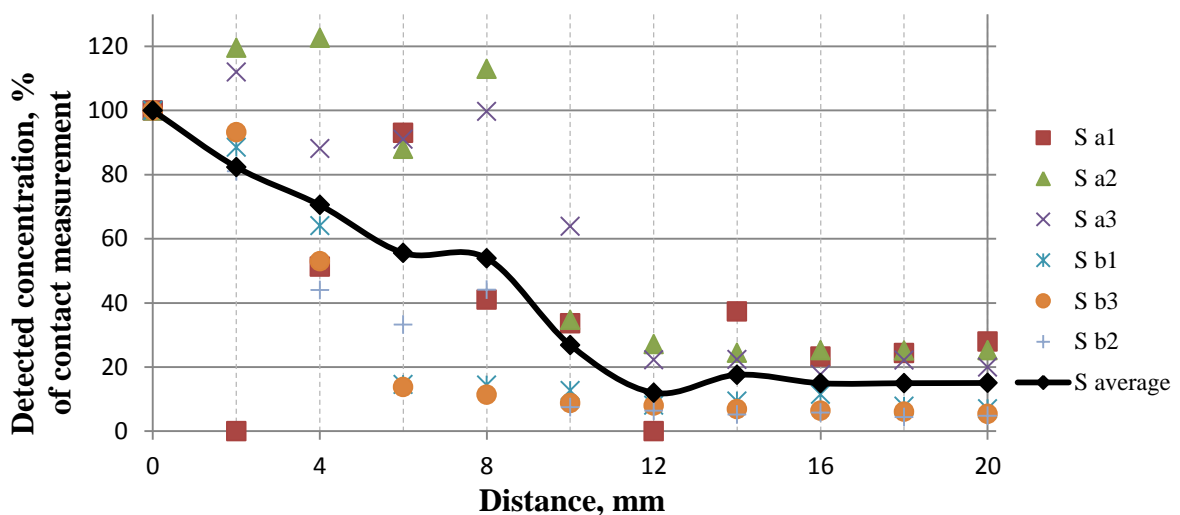
FIGURE 9. Dependence of detected S concentration on distance to sample, %
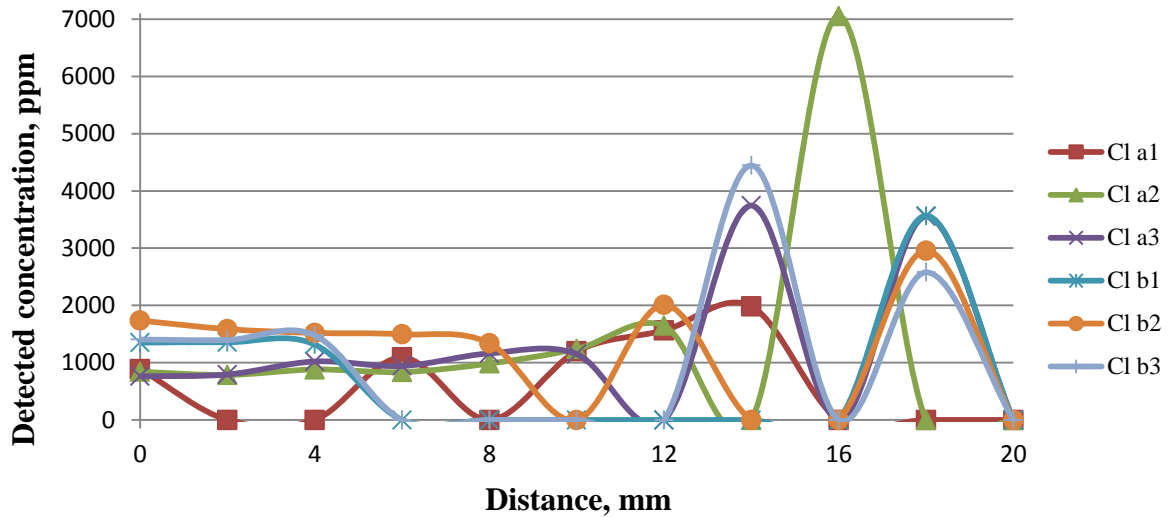
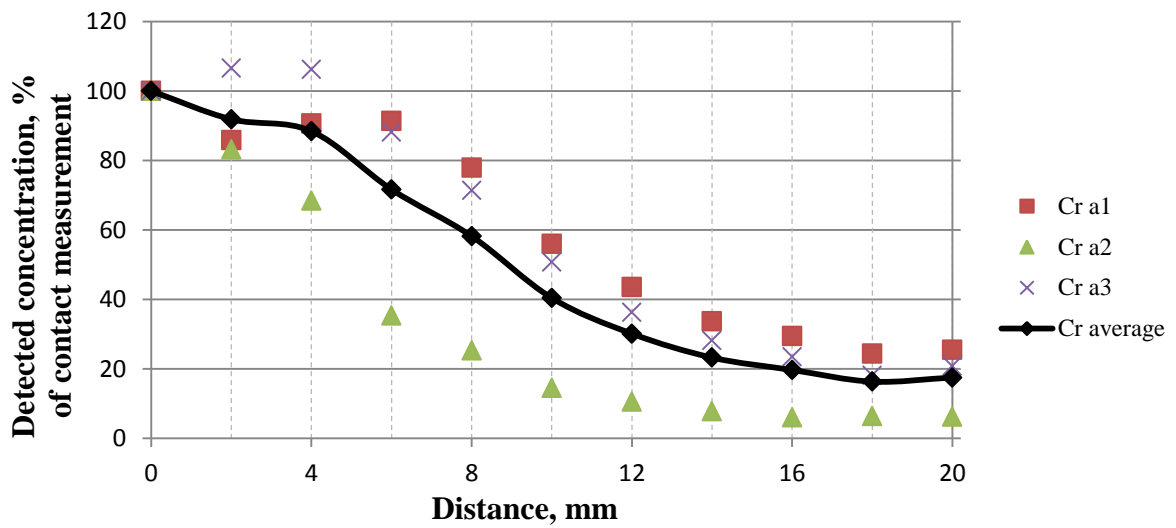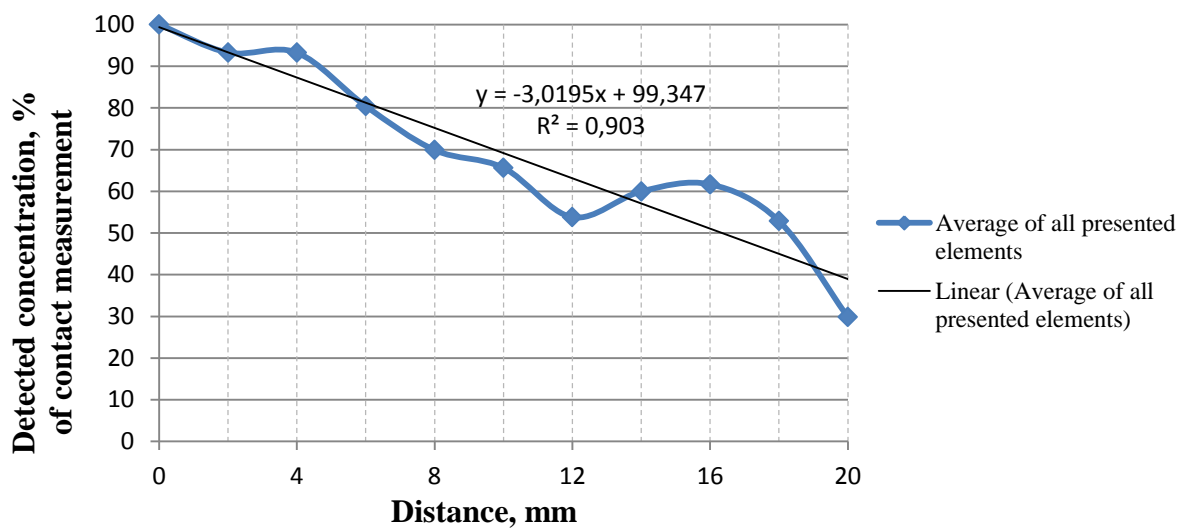**FIGURE 10. Dependence of detected Cl concentration on distance to sample, ppm**
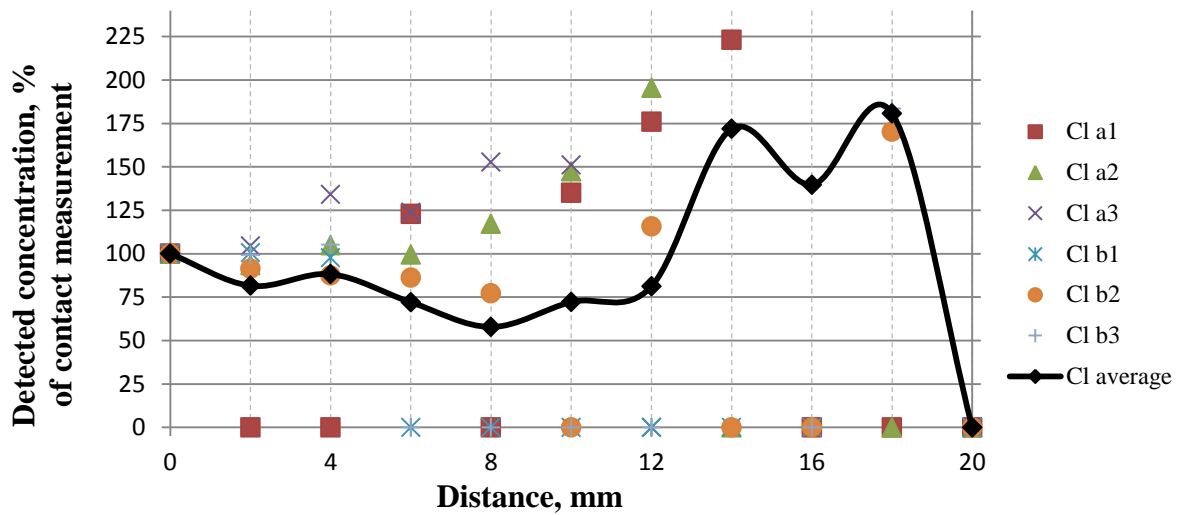
**FIGURE 11. Dependence of detected Cl concentration on distance to sample, %
(top part of figure removed; the highest value is 838 % for 'Cl a2' at 16 seconds)**
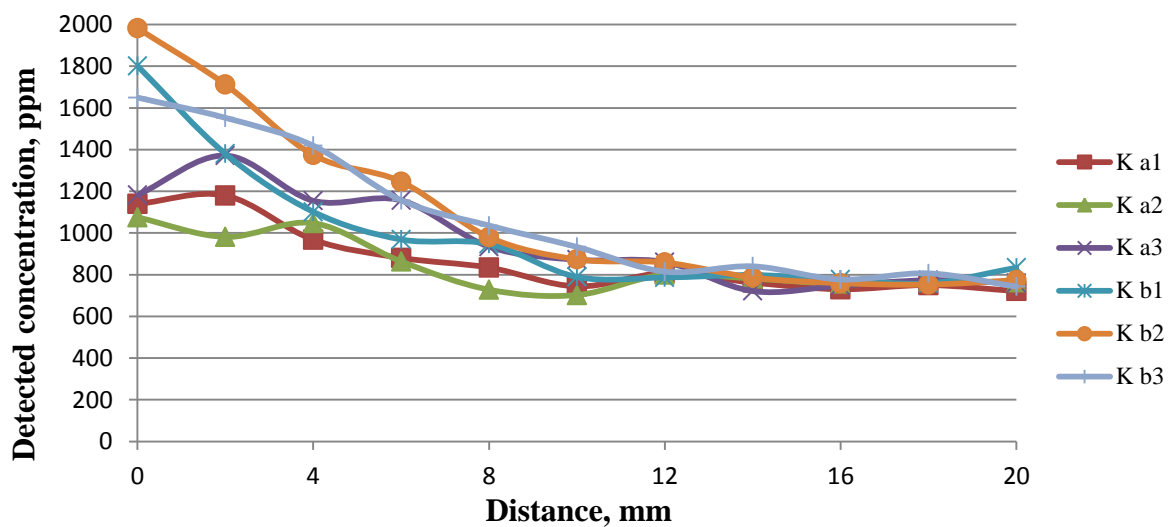
FIGURE 12. Dependence of detected K concentration on distance to sample, ppm
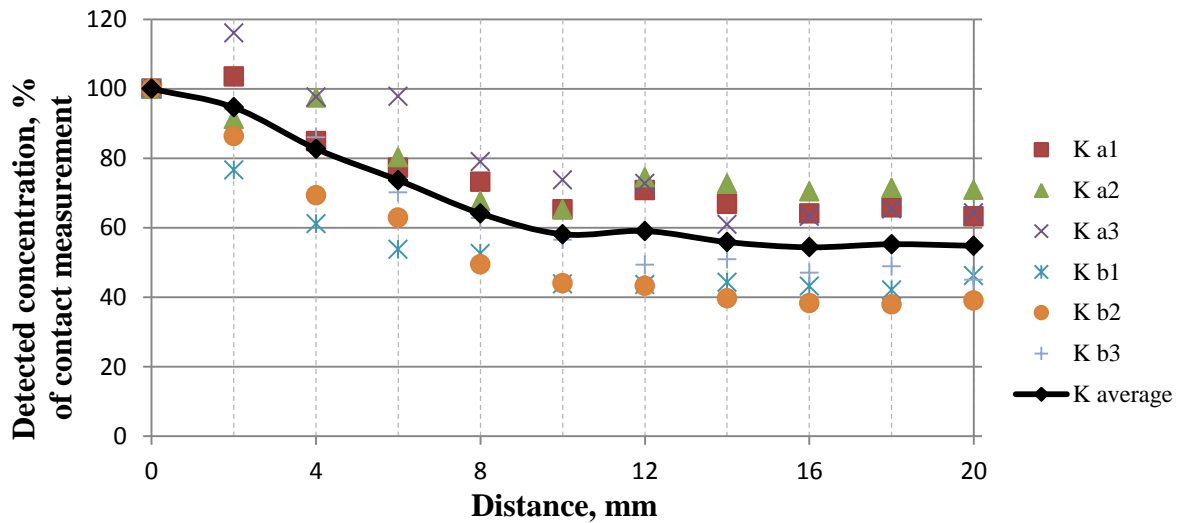
FIGURE 13. Dependence of detected K concentration on distance to sample, %
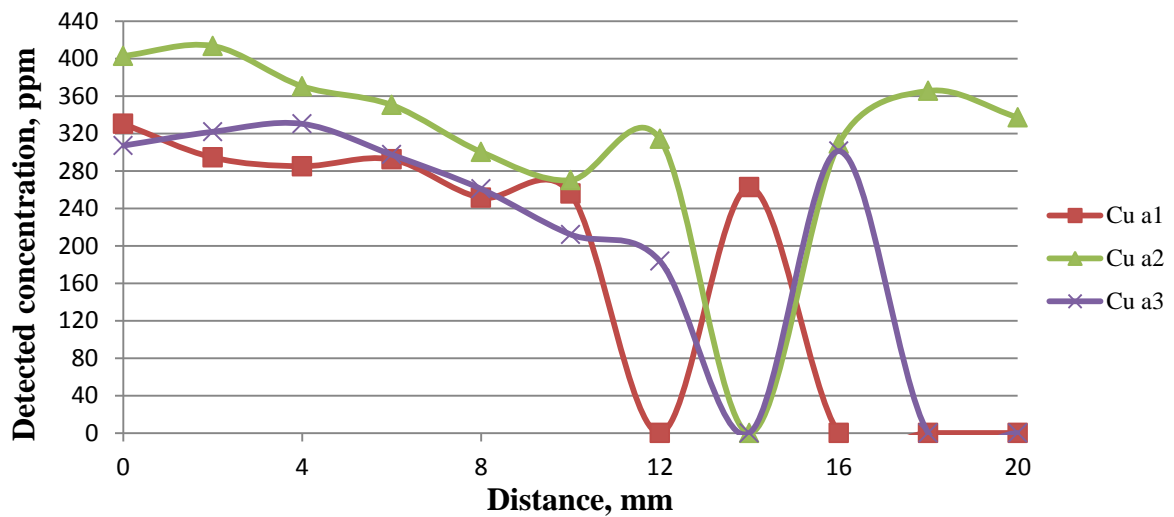
FIGURE 14. Dependence of detected Cu concentration on distance to sample, ppm
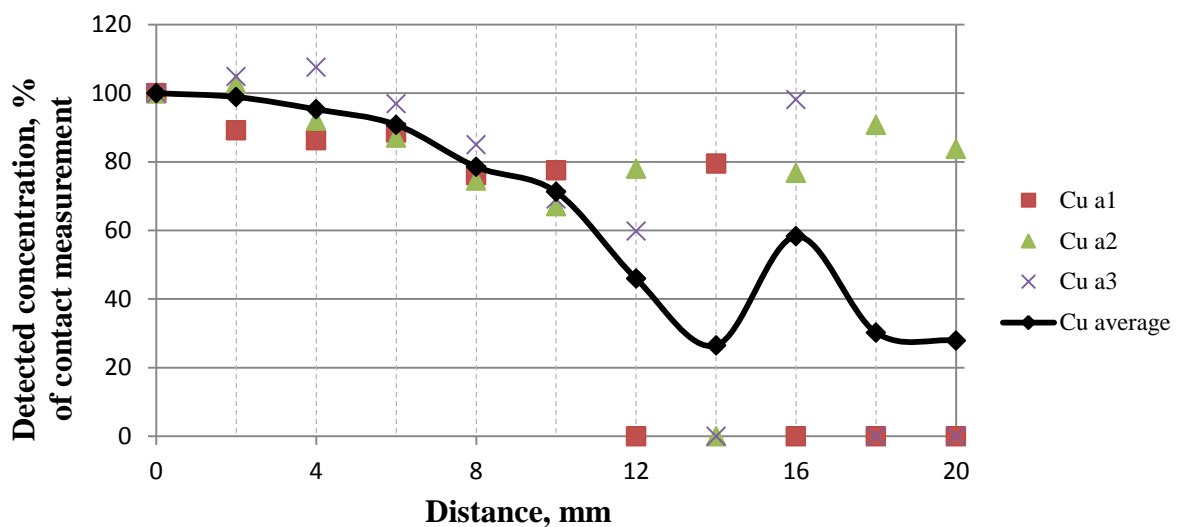
FIGURE 15. Dependence of detected Cu concentration on distance to sample, %
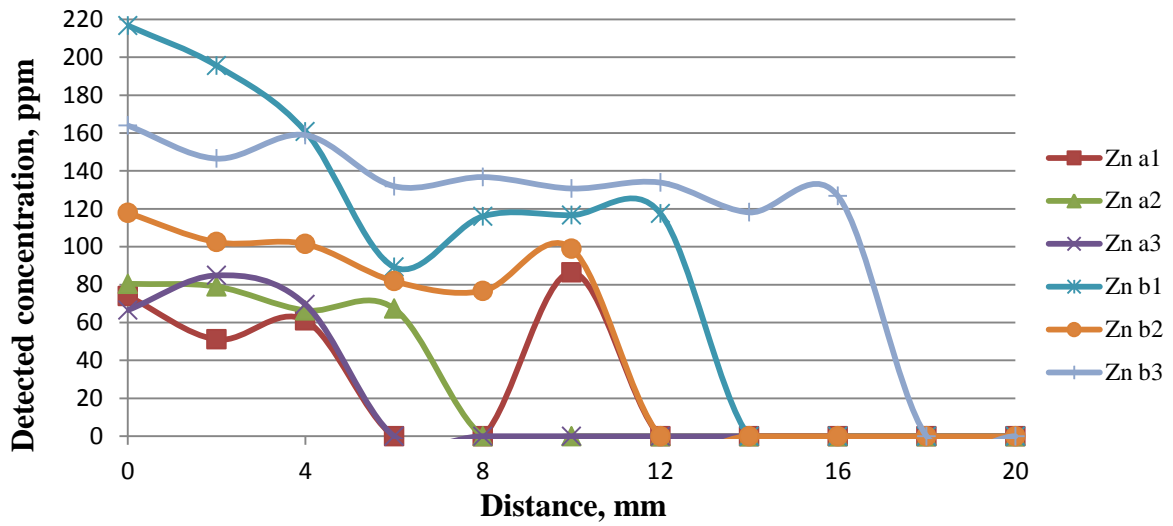
FIGURE 16. Dependence of detected Zn concentration on distance to sample, ppm
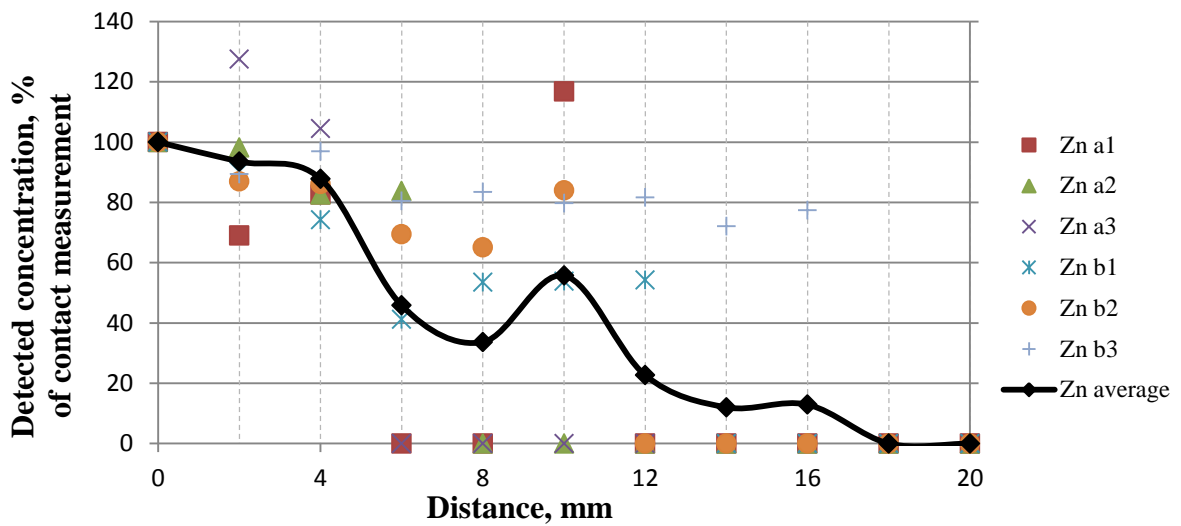
FIGURE 17. Dependence of detected Zn concentration on distance to sample, %
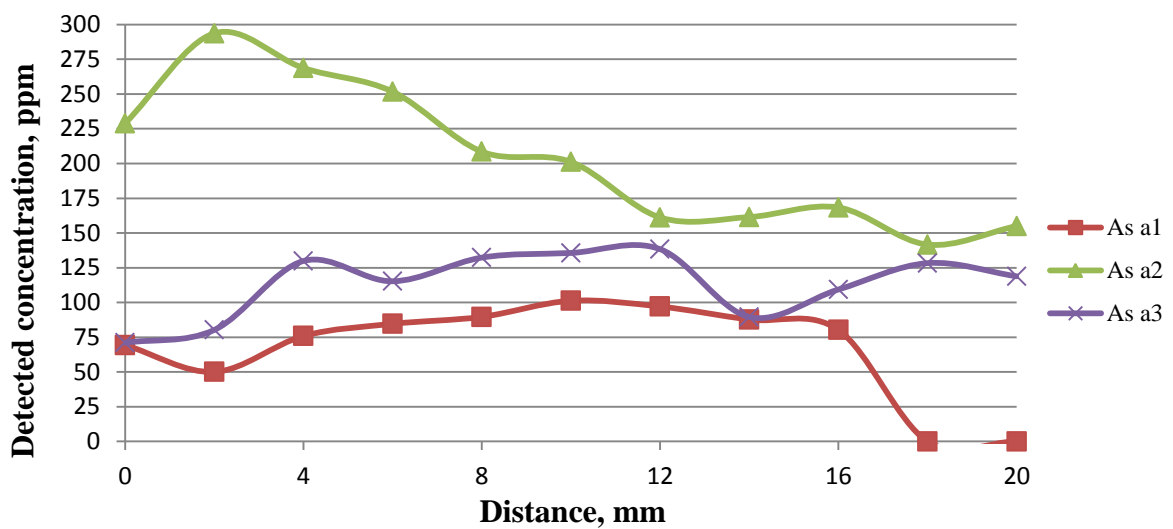
FIGURE 18. Dependence of detected As concentration on distance to sample, ppm
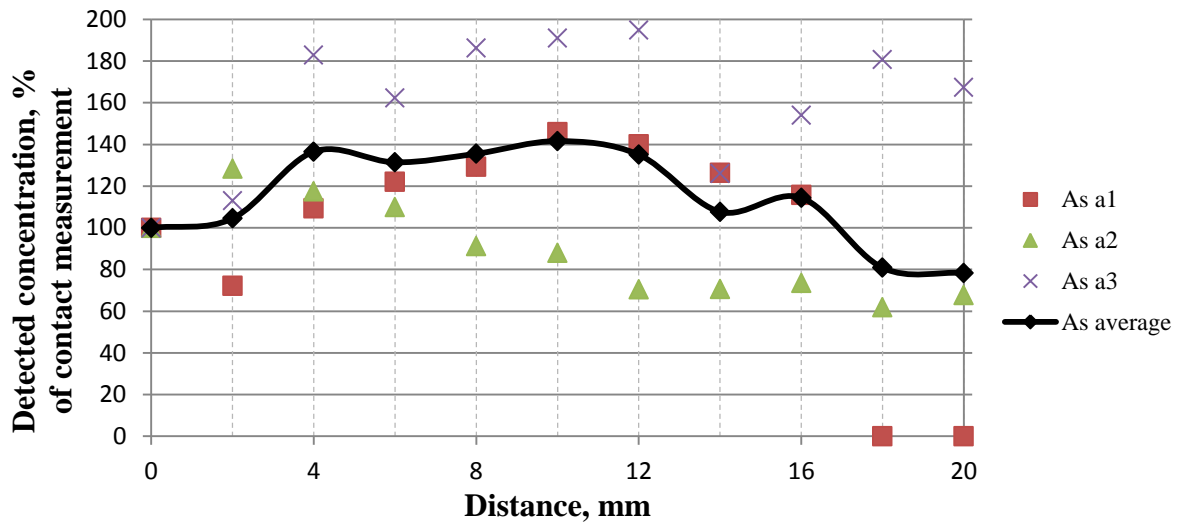
FIGURE 19. Dependence of detected As concentration on distance to sample, %
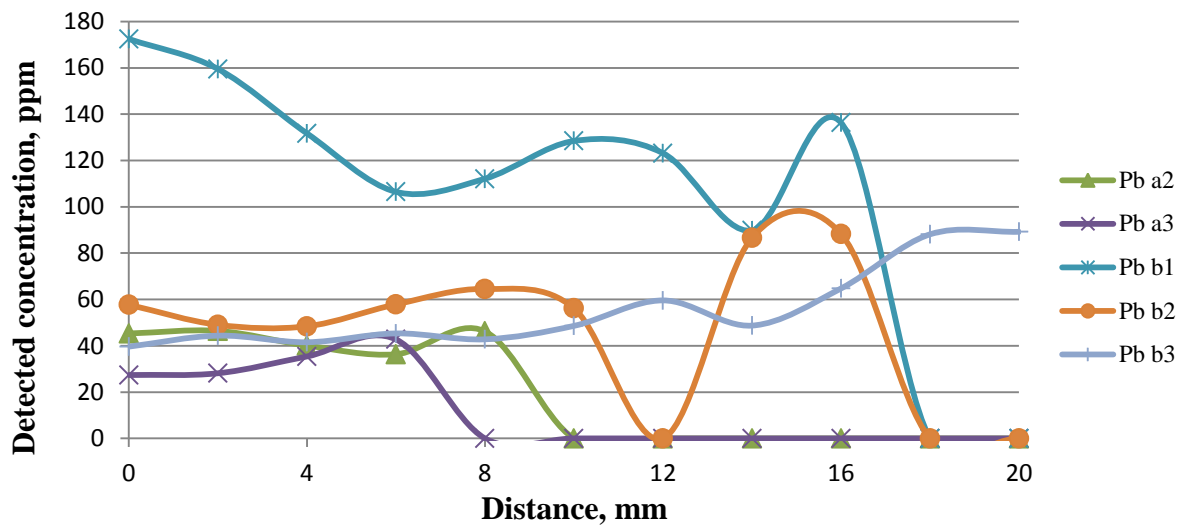
FIGURE 20. Dependence of detected Pb concentration on distance to sample, ppm
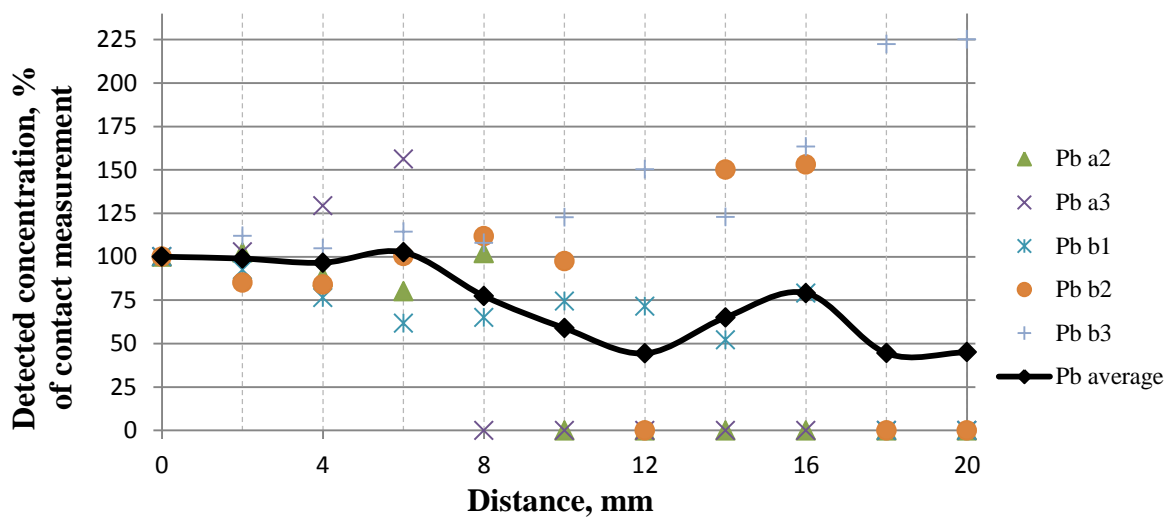
FIGURE 21. Dependence of detected Pb concentration on distance to sample, %

FIGURE 22. Dependence of detected Cr concentration on distance to sample, ppm

FIGURE 23. Dependence of detected Cr concentration on distance to sample, %

FIGURE 24. Dependence of detected elemental concentration on distance to sample, average of all presented elements (S, Cl, K, Cu, Zn, As, Pb, Cr)

Analysing the Figures 8 – 23 presented above, it can be seen that as a general trend, the detected concentrations fluctuated considerably between the measurements of same elements. The variations increased with increasing distance, especially above 6 mm. However, K and Cr had smooth trend lines. For As and Pb, at low original concentration value (at 0 mm distance) the detected concentrations increased with increasing distance; however at high original concentration values, their detected concentrations decreased with increasing distance. The average trend of all presented elements is illustrated in the Figure 24. It indicates that, generally from 0 mm to 12 mm, detected concentrations were proportional to the distance. However, detection of elements at a distance greater than 12 mm did not follow the trend.
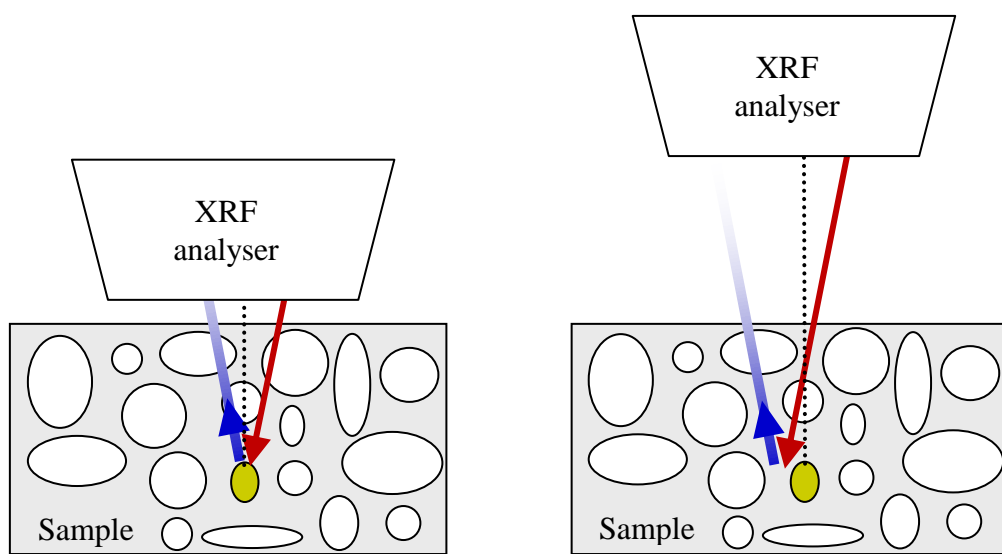
FIGURE 25. XRF analysis at different distances to sample

The observed fluctuations in the detected concentration values may be explained by several mechanisms that occurred during the conducted tests. Firstly, the increased air gap attenuated fluorescent photons, and it led to a reduced number of counts per second on the XRF detector, and thus, the detected concentrations. Secondly, compared to long analysis time, the short measurement time used in these tests produced greater errors. Moreover, even those concentration values received from the measurements taken for 5 seconds at the same distance sometimes differed considerably. Thirdly, because the demolition wood samples were highly heterogeneous, when the analyser was moved vertically, its primary X-ray beam could analyse a different particle inside the sample, as schematically shown in the Figure 25 above. Due to the fact that the X-ray source tube is fixed at an angel inside the analyser, moving the analyser vertically created a small displacement at the horizontal level of the initial measurement.

6.4   Wood moisture

The aim of this test was to find out if there was any possible correlation between the measured and real elemental concentrations in recovered wood and observe at what wood moisture levels the XRF-analyser stopped identifying elements. Two recovered wood samples of roughly 50 grams (dry mass) were prepared and soaked in distilled water for 10 days. The first sample labelled "a" was the ≤ 8 mm particles, and the second sample labelled "b" was the ≤ 31,5 mm particles grinded to particles of 6 mm in size. The moisture contents in the samples were raised to around 70 % and 80 % for the sample "a" and "b" respectively. The samples were dried in an oven at 105 °C and periodically taken for the XRF analysis.

Different spots (a1, a2, b1, b2, b3) of the samples were analysed during 5 seconds per element range. Two XRF measurements were taken per a spot. The samples were weighed before the XRF analysis and immediately after it. The average of these two mass values was used for calculating the moisture content. On average, 1 g of water evaporated during the analyses. A paper sheet with marked coordinates of the spots was used in order to constantly place the XRF-analyser above the spots.

The detected elemental concentrations were in ppm. However, the concentrations varied between the samples and spots considerably, as the example of Cl shows in the Figure 26 below. Because the aim of the test was to evaluate how moisture affected the XRF readings, all result values were converted to per cents of the measured concentration at 0 % moisture content. Therefore the detected elemental concentration at the 0 % moisture level was set to a 100 % elemental concentration, and the other measured elemental concentrations at different moisture levels were calculated as proportions to it.

This data presentation method allows easier comparison of the results regardless of their actual concentrations. For instance, the Figure 27 represents the same Cl values as the Figure 26 but in percentage. As a result, the relationship between the detected Cl concentration and the wood moisture content can be clearly seen regardless of the measured concentrations. Such a representation also helped to create the average dependence across all the XRF element measurements using statistical methods. The average trend was calculated up to 70 % of moisture level as it was the highest common moisture value for the samples "a" and "b".
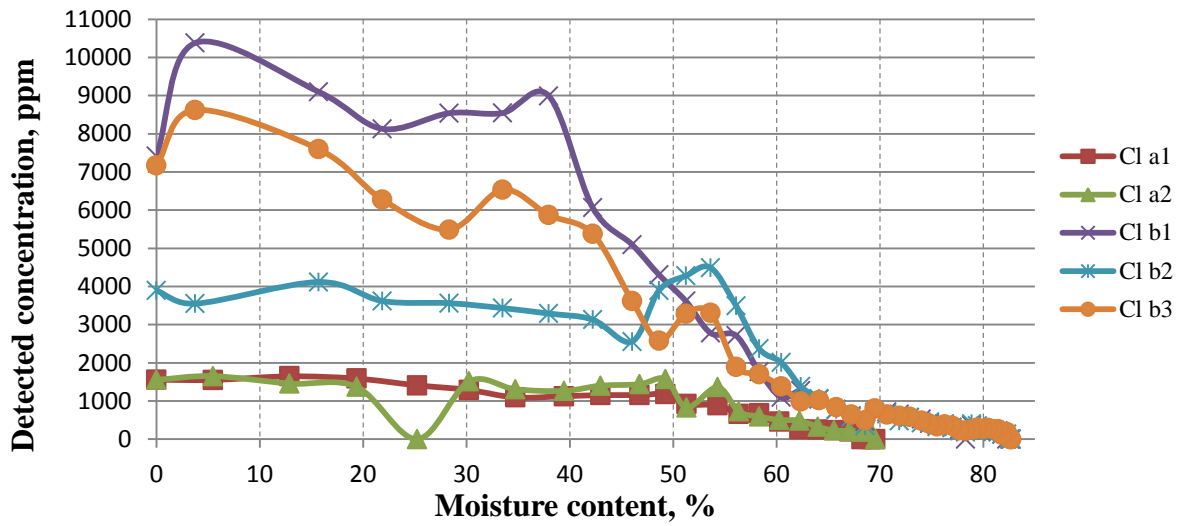
FIGURE 26. Dependence of detected Cl concentration on wood moisture content, ppm
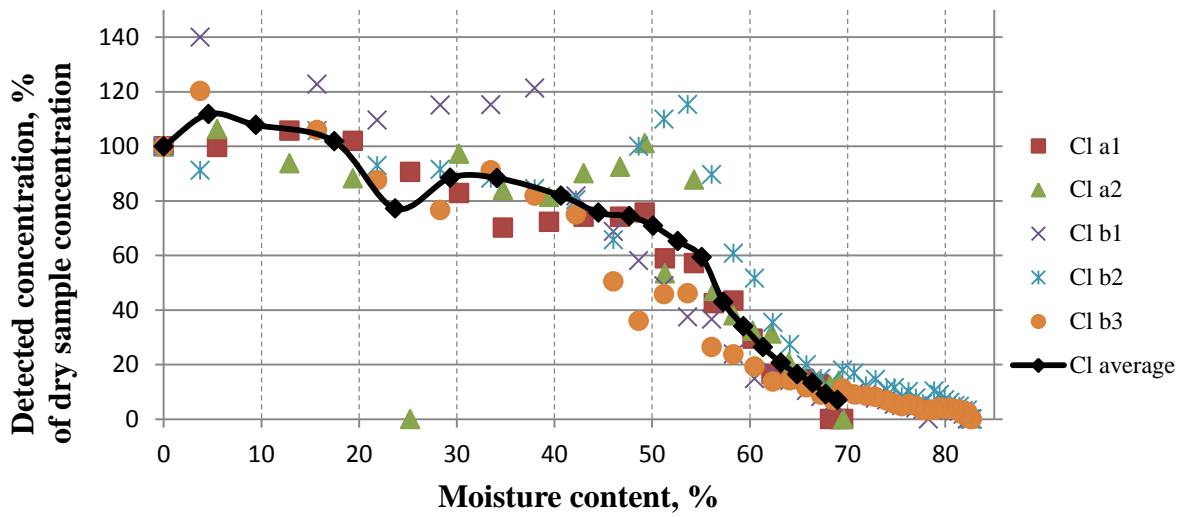

FIGURE 27. Dependence of detected Cl concentration on wood moisture content, %
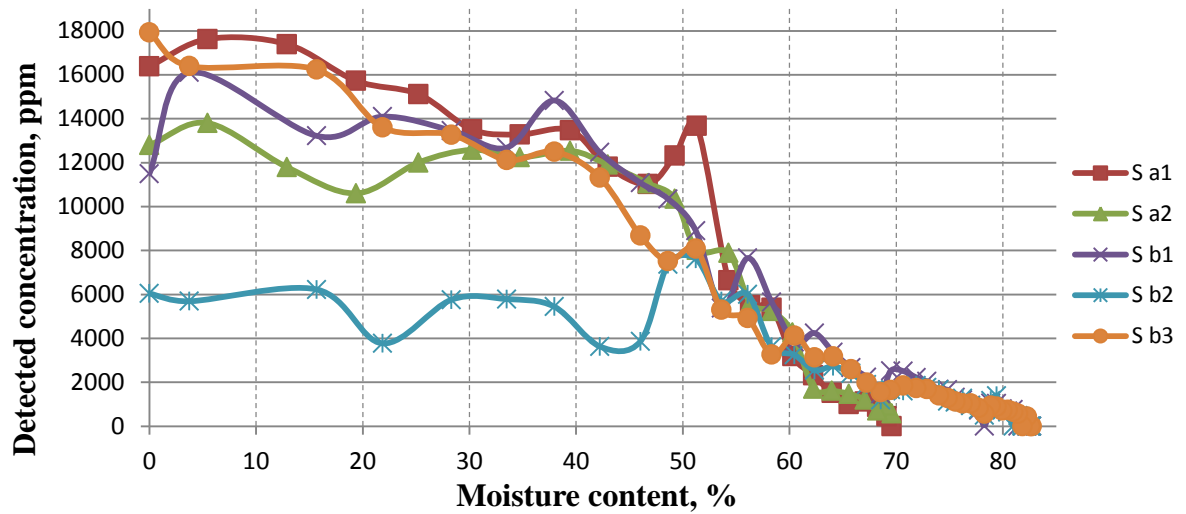

FIGURE 28. Dependence of detected S concentration on wood moisture content, ppm
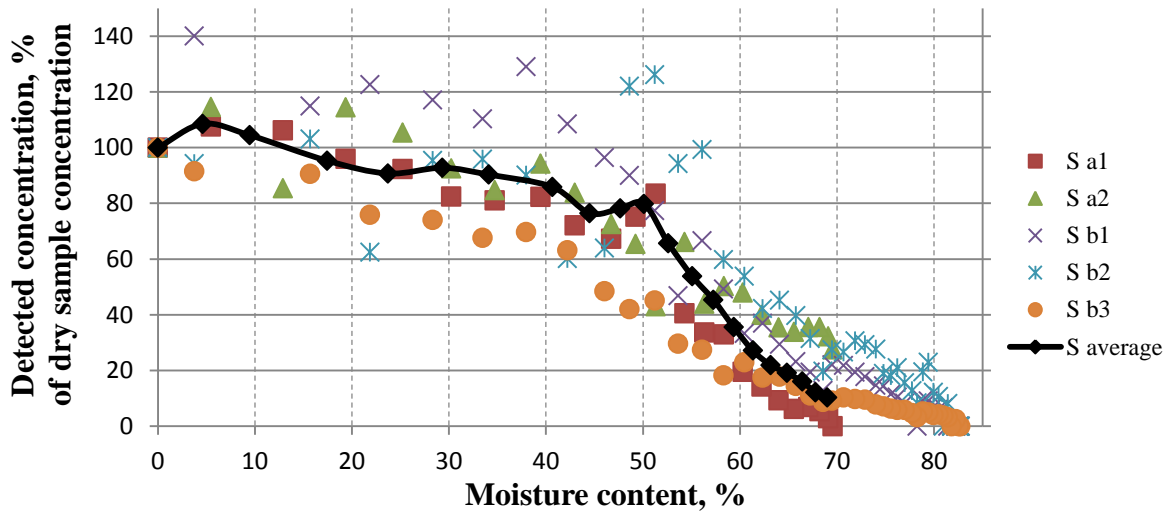
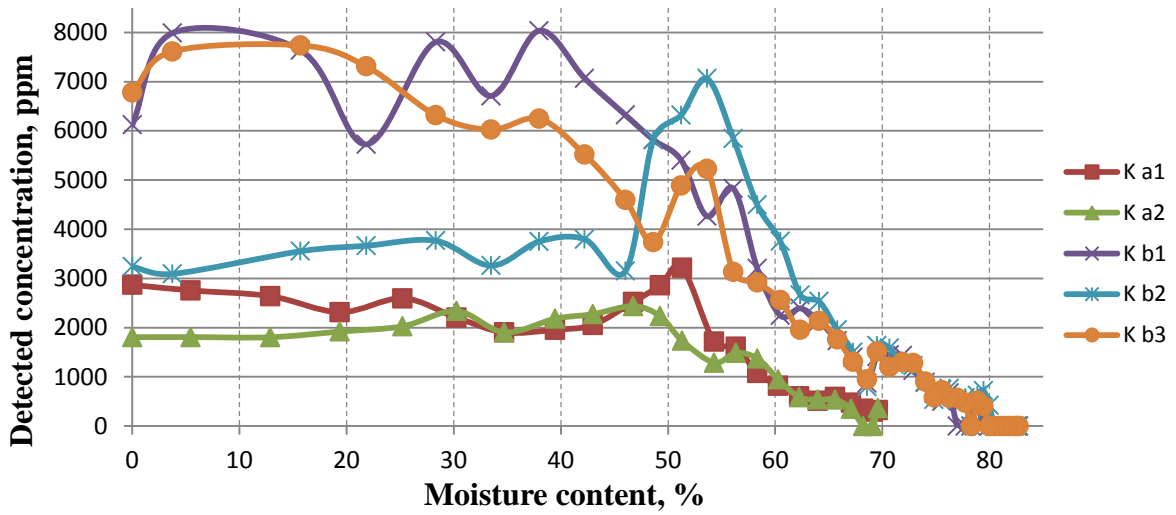**FIGURE 29. Dependence of detected S concentration on wood moisture content, %**

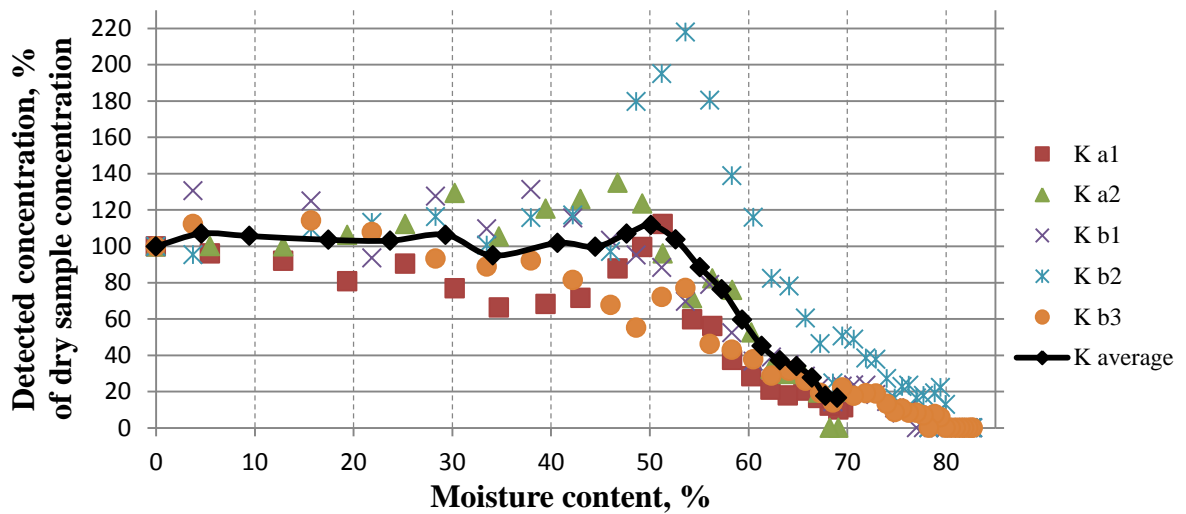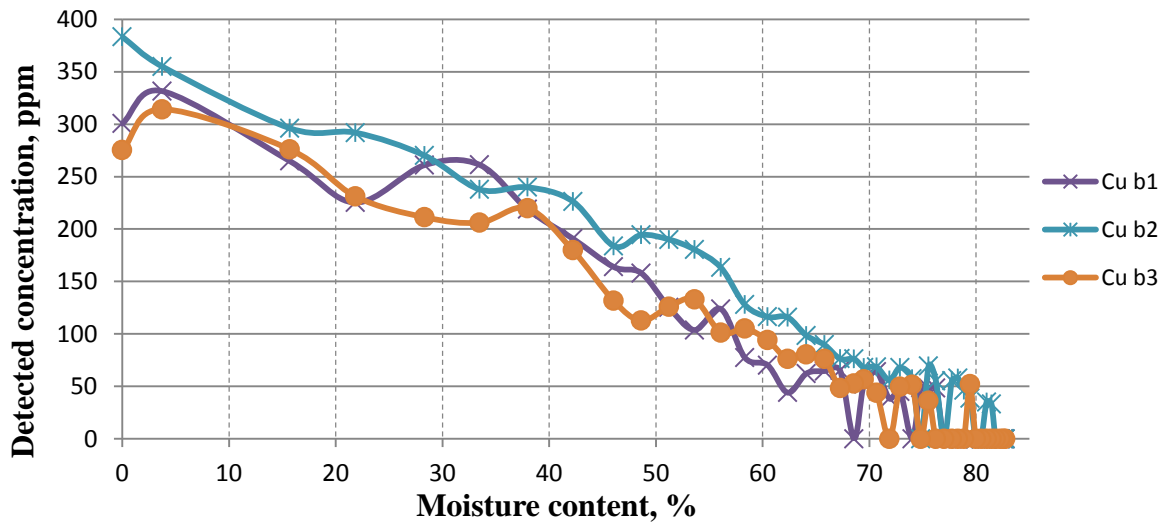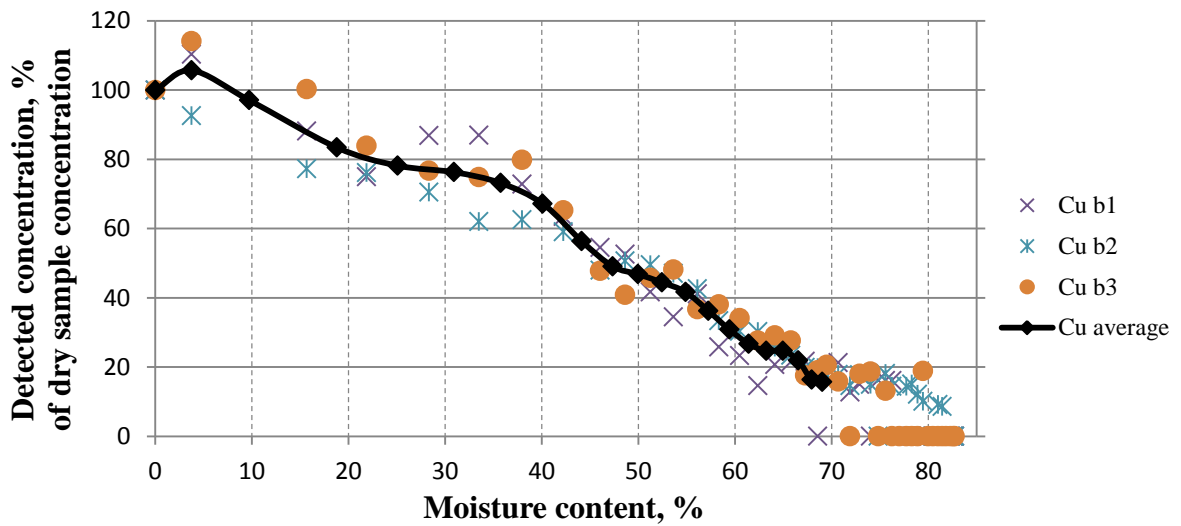**FIGURE 30. Dependence of detected K concentration on wood moisture content, ppm**

FIGURE 31. Dependence of detected K concentration on wood moisture content, %

FIGURE 32. Dependence of detected Cu concentration on wood moisture content, ppm

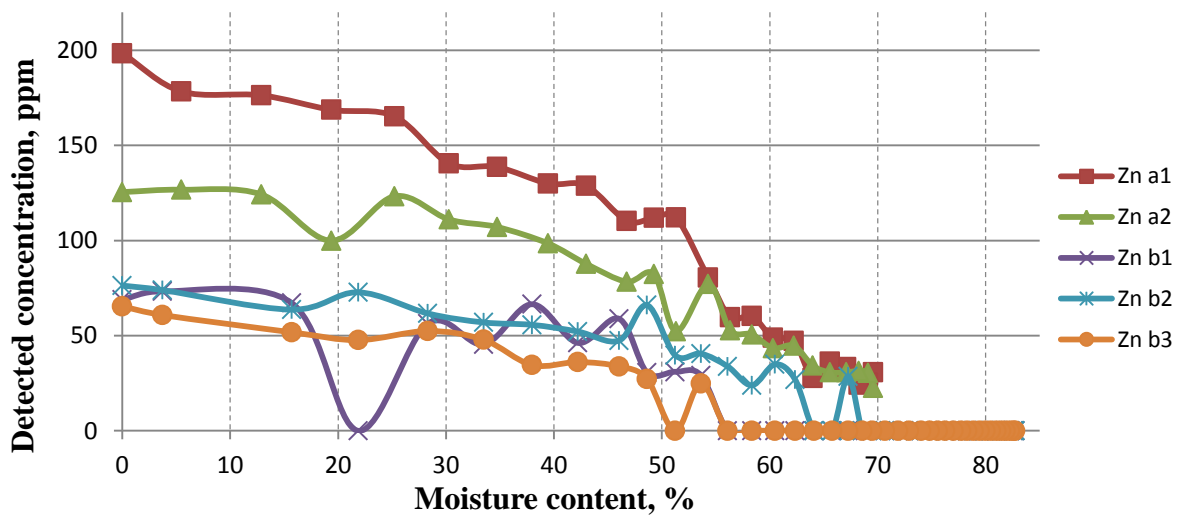FIGURE 33. Dependence of detected Cu concentration on wood moisture content, %

FIGURE 34. Dependence of detected Zn concentration on wood moisture content, ppm
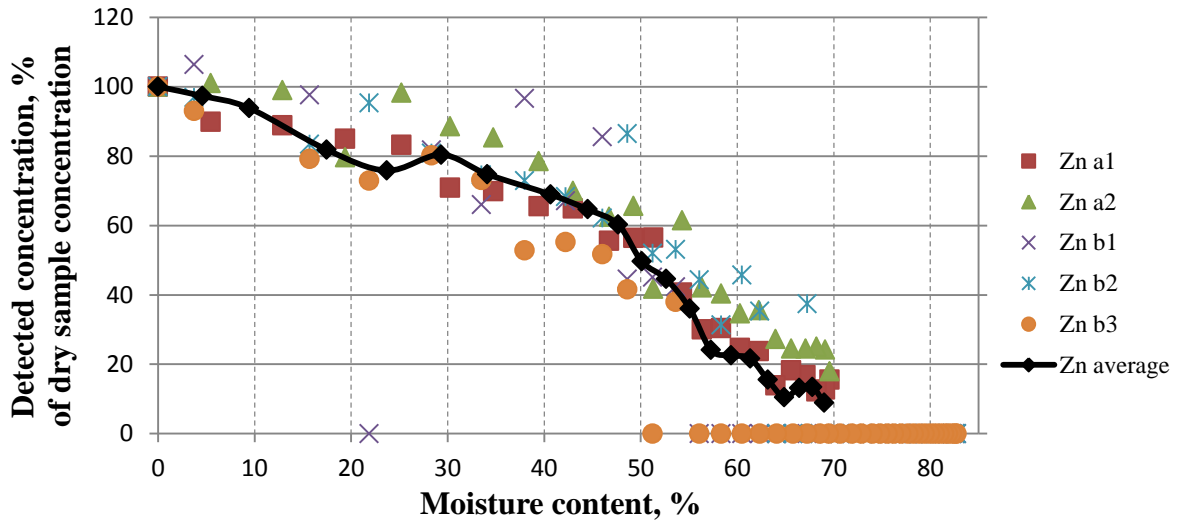
FIGURE 35. Dependence of detected Zn concentration on wood moisture content, %
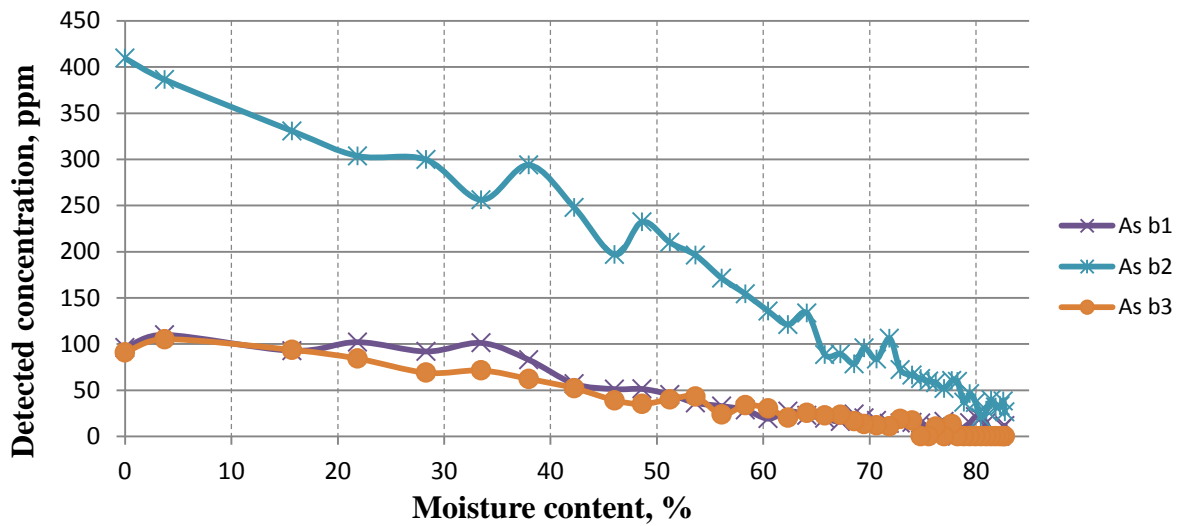

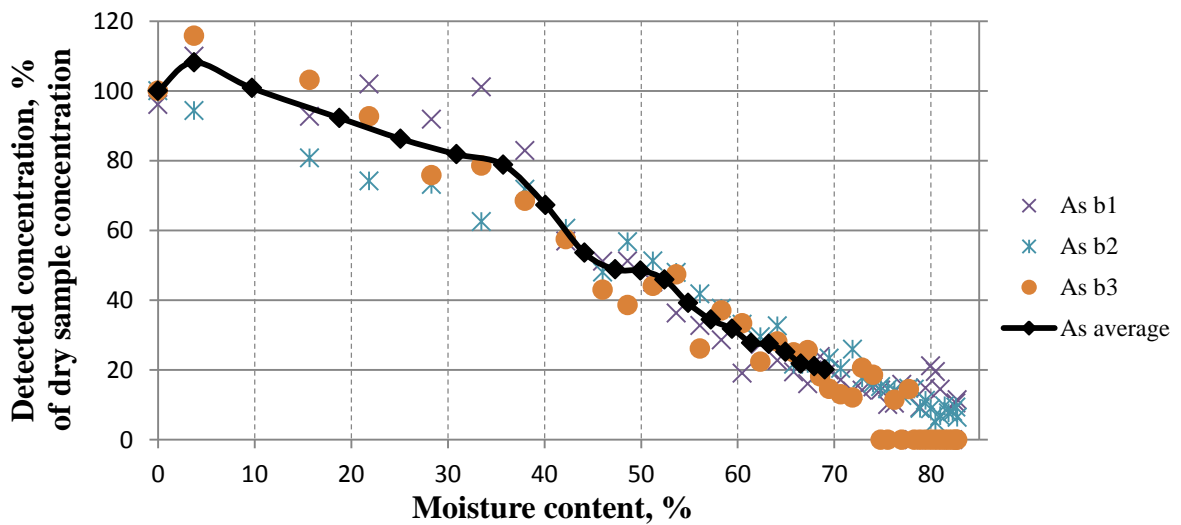FIGURE 36. Dependence of detected As concentration on wood moisture content, ppm

FIGURE 37. Dependence of detected As concentration on wood moisture content, %
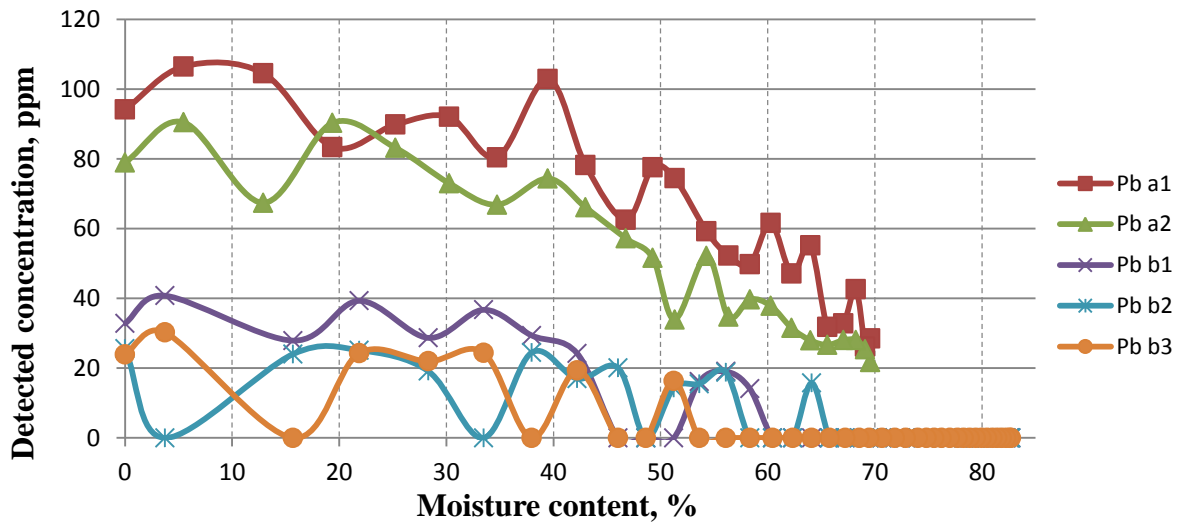
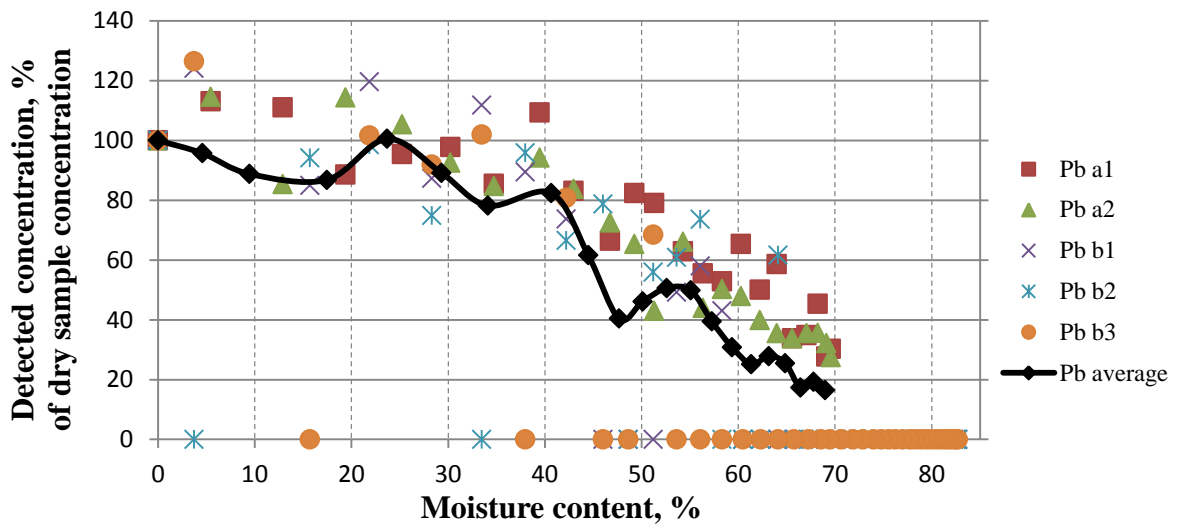**FIGURE 38. Dependence of detected Pb concentration on wood moisture content, ppm**

FIGURE 39. Dependence of detected Pb concentration on wood moisture content, %
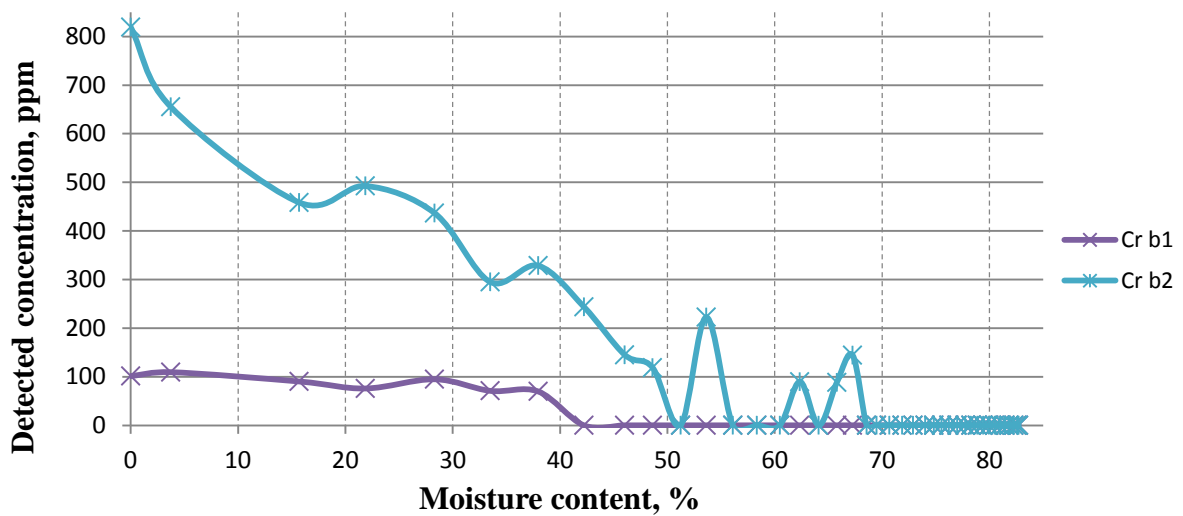

FIGURE 40. Dependence of detected Cr concentration on wood moisture content, ppm
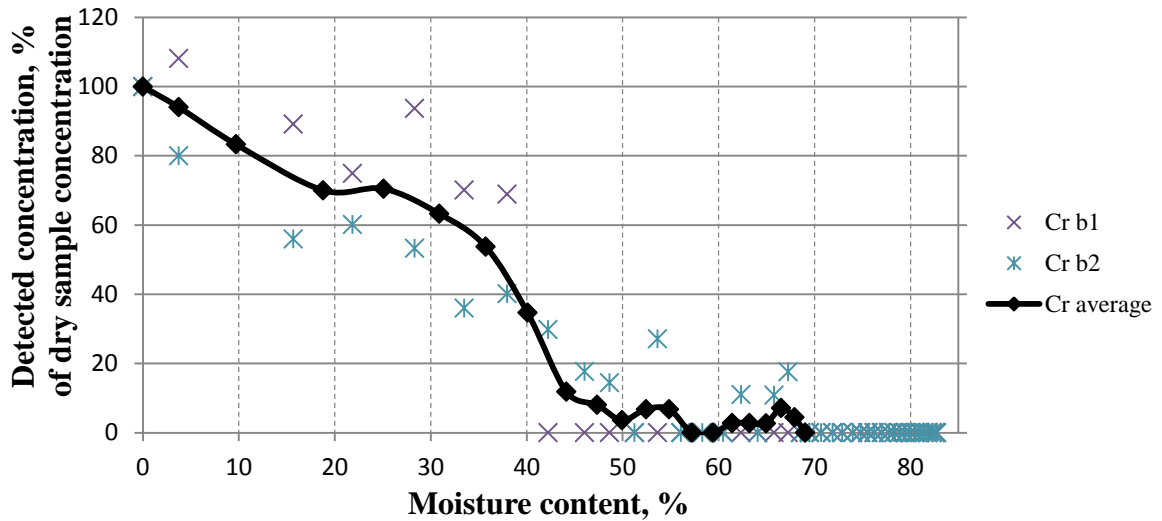
FIGURE 41. Dependence of detected Cr concentration on wood moisture content, %

Analysing the figures above, it can be noticed that regardless of the chemical element and its real concentration in wood, the measured concentrations were proportionally affected by wood moisture content. Increased moisture content lowered the detected concentrations. It was found that each element had its own correlation trend. In the case of K, the detected concentration remained at nearly the same level from 30 % to 0 % of wood moisture. For most of the presented elements, they were identified even at 70 % moisture content. However, elements in high concentrations are traced better at high moisture content than elements in low concentrations. The graph in the Figure 42 represents the average of moisture correlations of all presented above elements. This figure also shows an order 2 polynomial trend line closely fitted to the data which suggests a possibility for mathematical correction of results.
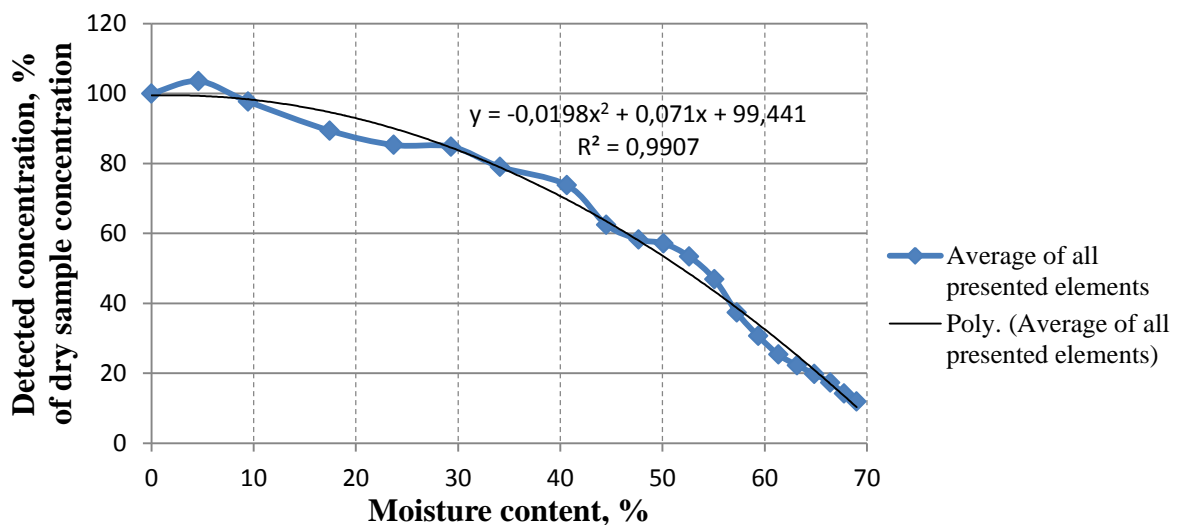

$$y = -0,0198x^2 + 0,071x + 99,441$$
$$R^2 = 0,9907$$

FIGURE 42. Dependence of detected elemental concentration on wood moisture content, average of all presented elements (S, Cl, K, Cu, Zn, As, Pb, Cr)

The results also showed high measured elemental concentration deviations during the course of the tests. These fluctuations were most likely to occur because of the short analysis time of 5 seconds and a minor shift of the analyser above the spots from analysis to analysis. Upon drying, the sample particles slightly shrank and enlarged the voids between them. It consequently displaced the particles from their original position in the sample. In some instances, elements were not detected even though they were detected in the previous and next measurements. It led to an increased fluctuation of the average correlation trend. However, these visual representations provided a good general estimate of how moisture affected the XRF elemental analysis results.

6.5   Radiation safety

Although a backscatter shield was used, it did not protect from radiation that comes sideways during XRF analysis of wood chips. For intended laboratory work timeframe, the radiation dose rates of the Niton XL3t 980 GOLDD+ handheld XRF-analyser were found to exceed the legal radiation limits set by the Finnish authorities. The Table 17 below shows the radiation measurement results.

TABLE 17. Radiation dose rates at different distances, "main" range in Soil mode

Distance from sample	Radiation dose rate without air gap, µSv/h		Radiation dose rate with 2 cm air gap, µSv/h	
	Typical	Max observed	Typical	Max observed
1 cm	26,2 - 32,2	39,9	27,3 - 37,8	39,1
40 cm	2,88 - 3,09	3,45	2,58 - 3,36	3,84
80 cm	0,77 - 0,90	1,50	0,72 - 0,82	0,86
120 cm	0,25 - 0,37	0,50	0,39 - 0,44	0,48

The background radiation in the room was in a range of 0,08 – 0,14 µSv/h. Radiation rate was also measured under the experiment table below the XRF-analyser (see the Picture 1 in the chapter 5 "Methods used in this study"). Even though there were layers of the analysed sample, metal jack stand, wooden stand used to fix the analyser, and the table, the dose rates were 50,4 – 65,5 µSv/h under the table. When radiation levels were measured in contact with the analyser, directly under it, the radiation meter immediately gave an error, most likely because its maximum detection limit of 100 000 µSv/h was exceeded.

PICTURE 4. Experimental set-up for XRF-analyser with lead shielding

In order to illuminate the unwanted radiation which was scattered from samples during analyses, the test equipment was shielded with several 2 mm lead plates as seen in the Picture 4 above. As a result, the radiation was completely absorbed, and at any distance from the shielding the radiation meter showed only the background radiation dose. This set-up was used for all measurements of recovered wood samples.

7 CONCLUSIONS

The results of the practical tests during this thesis project showed consistency with previous studies on XRF analysis, particularly, that moisture, air gap and short measurement time negatively affected the detected elemental concentrations. However, the literature review provided only general information, for example, that moisture reduced XRF detectability of elements without any given correlations. This thesis presented valuable and more detailed information on the limitations of XRF analysis. Moreover, now the data is available for specific challenging elements in recovered wood fuel.

The literature review and practical work showed that analysis of wood with XRF equipment was challenging due to its limitations, however it was practically feasible. Understanding of limiting conditions and their effects on the XRF analysis results should improve accuracy of solid fuel quality control with a handheld XRF-analyser. Recommendations for better measurements are provided below. This study was made with a Niton XL3t 980 GOLDD+.

Firstly, the shortest and yet accurate analysis time for wood samples is 30 seconds per element range, or 2 minutes per full analysis. Secondly, a contact measurement with a sample is most desirable. Thirdly, wood moisture lowers detected elemental concentrations, however it is possible to mathematically correct the measured values when knowing the moisture content. Lastly, it was found that the small recovered wood particles (4 mm and less) contained high concentrations of contaminating elements. Therefore, it is advisable to illuminate them prior combustion.

It should be noted that results of XRF analysis represent only a very small part of a sample. One way to improve the accuracy is to make more measurements. Ultimately, an online XRF measurement system could be a solution to this issue as it would scan wood chips continuously on a moving conveyor.

With regards to an online XRF system, it should be able to analyse all ranges of elements, including light and heavy elements, without the need to switch between the element ranges. It would increase the processing speed and thus the amount of analysed material on a conveyer. The XRF detector of the online measurement system should not be located further than 12 mm above the sample as the air gap attenuates XRF photons and drastically reduces the

detected elemental concentration. Also, this system should have a cooling system because the XRF-analyser overheats during long measurements and does not allow working until it has cooled down.

Lastly, further studies should be organised for more detailed research on XRF performance in recovered wood quality control. Particularly for an online XRF system, a high number of tests is needed to create accurate correlation formulas for effects of wood moisture on the XRF analysis results. Dependence of measured elemental concentrations on elevation distance above wood samples should be further explored for possible usable correlation formulas. Finally, performance of the XRF-analyser over moving samples should be studied as a simulation of a working conveyer belt.

In the conclusion, the studied XRF analyser can be used in solid biofuel quality control. It is capable of identifying the elements listed in the EU biofuel standards and specifications, except for N and Na. The XRF analysis is fast and accurate, and its precision can be further increased with mathematical corrections of negative effects of known limitations. The elemental XRF analysis with the handheld XRF-analyser can be performed by personnel without a background in physics or chemistry. However, personal radiation safety must be ensured when analysing wood samples due to high radiation dose rates near the analyser.

REFERENCES

Amptek Inc. What is XRF?. WWW-document. http://www.amptek.com/xrf/. No update information. Referred 22.4.2015.

Anzelmo, John, Bouchard, Mathieu & Provencher Marie-Eve 2014. X-ray fluorescence spectroscopy, part II: sample preparation. Spectroscopy magazine. Volume 29 Number 7. PDF document. http://images2.advanstar.com/PixelMags/spectroscopy/pdf/2014-07.pdf. No update information. Referred 22.4.2015.

Bankiewicz, Dorota 2012. Corrosion behaviour of boiler tube materials during combustion of fuels containing Zn and Pb. Academic dissertation. PDF document. https://www.doria.fi/bitstream/handle/10024/77050/bankiewicz_dorota.pdf?sequence=2. No update information. Referred 22.4.2015.

Bruker 2008. Draft Bruker XRF spectroscopy user guide: spectral interpretation and sources of interference. PDF document. http://www.ifuap.buap.mx/Workshop-XRF/XRF-theory/Bruker_Tracerand_Artax_XRF_Raw_Spectrum_Analysis_User_.pdf. Updated 11.11.2008. Referred 22.4.2015.

Bruker 2012. EDX vs WDX: Head to Head. PDF document. http://www.bruker.com/fileadmin/user_upload/8-PDF-Docs/X-rayDiffraction_ElementalAnalysis/XRF/Webinars/Bruker_AXS_EDX_vs_WDX_Webinar_Slides.pdf. Updated 18.4.2012. Referred 22.4.2015.

Bruker. Periodic table of elements and X-ray energies. PDF document. http://www.bruker.com/fileadmin/user_upload/8-PDF-Docs/X-rayDiffraction_ElementalAnalysis/HH-XRF/Misc/Periodic_Table_and_X-ray_Energies.pdf. No update information. Referred 22.4.2015.

European recovered fuel organisation. Information document on EN 15359 "Solid recovered fuels – specifications and classes". PDF document. http://erfo.info/fileadmin/user_upload/erfo/documents/reports/Information_document_EN15359.pdf. No update information. Referred 22.4.2015.

Fellin, Marco, Negri, Martino, Mazzei, Federico & Zanuttini, Roberto 2014. Characterization of ED-XRF technology applied to wooden matrix. Wood research. PDF document. http://www.centrumdp.sk/wr/201404/02.pdf. No update information. Referred 22.4.2015.

Finnish radiation and nuclear safety authority 2008. Use of control and analytical X-ray apparatus. PDF document. http://www.finlex.fi/data/normit/35279-ST5-2e.pdf. No update information. Referred 22.4.2015.

Glanzman, R. & Closs, L. 2007. Field portable X-ray fluorescence geochemical analysis – its contribution to onsite real-time project evaluation. PDF document. http://www.dmec.ca/ex07-dvd/E07/pdfs/15.pdf. No update information. Referred 22.4.2015.

Guthrie, James 2012. Overview of X-ray fluorescence. WWW-document. http://archaeometry. missouri.edu/xrf_overview.html. Updated 21.11.2014. Referred 22.4.2015.

International renewable energy agency 2014. Global bioenergy: supply and demand projections. PDF document. http://irena.org/remap/IRENA_REmap_2030_Biomass_ paper_2014.pdf. No update information. Referred 22.4.2015.

ISO 17225-1:2014. Solid biofuels. Fuel specifications and classes. Part 1: general requirements. International standard.

Jones, Frida 2013. Characterisation of waste for combustion – with special reference to the role of zinc. Doctoral thesis. PDF document. https://www.doria.fi/bitstream/handle/ 10024/93783/jones_frida.pdf?sequence=2. No update information. Referred 22.4.2015.

Merlini, Mattia 2013. Classification and specification of SRF according to EN 15359 and overview of the European standards developed by CEN/TC 343 "Solid recovered fuels" PDF document. http://www.ieabioenergytask36.org/vbulletin/attachment.php?attachmentid =357&d=1385465332. No update information. Referred 22.4.2015.

Nakhaei F., Sam A. & Mosavi MR 2012. Prediction of XRF analyzers error for elements on-line assaying using Kalman filter. WWW-document. http://www.sciencedirect.com/science /article/pii/S2095268612001371. No update information. Referred 22.4.2015.

PAS 111:2012. Specification for the requirements and test methods for processing waste wood. Waste and Resources Action Programme. PDF document. http://www.woodrecyclers.org/PAS111.pdf. No update information. Referred 22.4.2015.

Sandberg, Jan 2011. Fouling in biomass fired boilers. Doctoral thesis. PDF document. http://www.diva-portal.org/smash/get/diva2:452326/FULLTEXT02. No update information. Referred 22.4.2015.

Solo-Gabriele, Helena, Townsend, Timothy, Hahn, David, Hosein, Naila, Jacobi, Gary, Jambeck, Jenna, Moskal, Tom & Kenjiro, Iida 2001. On-line sorting technologies for CCA-treated wood. PDF document. http://www.dep.state.fl.us/waste/quick_topics/publications /shw/recycling/InnovativeGrants/IGyear3/finalreports/sarasota.pdf. No update information. Referred 22.4.2015.

Solo-Gabriele, Helena, Townsend, Timothy, Hahn, David, Moskal, Thomas, Hosein, Naila, Jambeck, Jenna & Jacobi, Gary 2003. Evaluation of XRF and LIBS technologies for on-line sorting of CCA-treated wood waste. WWW-document. http://www.sciencedirect.com/science /article/pii/S0956053X03002058. No update information. Referred 22.4.2015.

Thermo Fisher Scientific Inc 2009. Mining FAQ. PDF document. http://www.us-tech.co.za/ downloads/thermo/Mining%20FAQs%202009Sept.pdf. No update information. Referred 22.4.2015.

Thermo Fisher Scientific Inc 2010. XL3 analyzer. User guide. PDF document. http://www. tttenviro. com/wp-content/uploads/Manual-XL3-Series-v7.0.11.pdf. No update information. Referred 22.4.2015.

Thermo Fisher Scientific Inc 2013. XRF technology for non-scientists. PDF document. http://www.thermoscientific.com/content/dam/tfs/ATG/CAD/CAD%20Marketing%20Materia l/CAD%20Marketing%20Documents/PAI%20Documents/TS-eBook-XRF-Technology-in-the-Field.pdf. No update information. Referred 22.4.2015.

Thermo Fisher Scientific Inc 2014. X-ray tube radiation survey certificate.

Thermo Fisher Scientific Inc. Thermo Scientific Niton XL3t GOLDD+ Specifications. PDF document. http://www.niton.com/docs/literature/Niton_XL3t_GOLDD_Spec_Sheet.pdf ?sfvrsn=2. No update information. Referred 22.4.2015.

US Environmental Protection Agency 2004. X-ray fluorescence instruments - frequently asked questions. PDF document. http://www.epa.gov/superfund/health/contaminants/lead /products/xrffaqs.pdf. Updated 25.5.2004. Referred 22.4.2015.

Vainikka, Pasi 2011. Occurrence of bromine in fluidised bed combustion of solid recovered fuel. Academic dissertation. PDF document. http://www2.vtt.fi/inf/pdf/publications /2011/P778.pdf. No update information. Referred 22.4.2015.

Vakkilainen, Esa, Kuparinen, Katja & Heinimö, Jussi 2013. Large industrial users of energy biomass. Report for IEA Bioenergy Task 40. PDF document. http://www.bioenergytrade.org/ downloads/t40-large-industrial-biomass-users.pdf. No update information. Referred 22.4.2015.

Valmari, Tuomas 2000. Potassium behaviour during combustion of wood in circulating fluidised bed power plants. Academic dissertation. PDF document. http://lib.tkk.fi/Diss/2000/ isbn9513855708/isbn9513855708.pdf. No update information. Referred 22.4.2015.

Viklund, Peter 2013. Superheater corrosion in biomass and waste fired boilers. Characterisation, causes and prevention of chlorine-induced corrosion. Doctoral thesis. PDF document. http://www.diva-portal.org/smash/get/diva2:614735/INSIDE01.pdf. No update information. Referred 22.4.2015.

Waste and Resources Action Programme 2009. Automated sorting of treated wood waste. PDF document. http://www2.wrap. org.uk/downloads/MDD015_Final_Report_ 11.03.10.7afca182.9756.pdf. No update information. Referred 22.4.2015.

Wobrauschek, Peter, Streli Christina & Lindgren, Eva Selin 2010. Energy Dispersive, X-ray Fluorescence Analysis. Encyclopedia of Analytical Chemistry R.A. Meyers. PDF document. http://publik.tuwien.ac.at/files/PubDat_187656.pdf. No update information. Referred 22.4.2015.